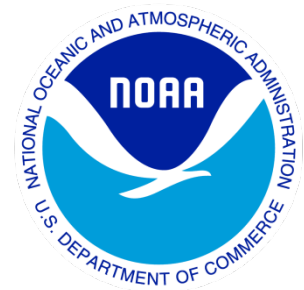

Climate Data Record (CDR) Program

Climate Algorithm Theoretical Basis Document (C-ATBD)

Outgoing Longwave Radiation – Monthly



CDR Program Document Number: CDRP-ATBD-0097
Configuration Item Number: 01B-06
Revision 5 / April 28, 2025

A controlled copy of this document is maintained in the CDR Program Library.
Approved for public release. Distribution is unlimited.

REVISION HISTORY

Rev.	Author	DSR No.	Description	Date
1	Hai-Tien Lee, CICS/UMD	DSR-102	Initial submission to CDR Program	09/01/2011
2	Hai-Tien Lee, CICS/UMD	DSR-586	Change made per CDRP-CR-0011	12/16/2013
3	Hai-Tien Lee, CICS/UMD	DSR-597	Change made per CDRP-CR-0029	01/03/2014
4	Hai-Tien Lee, CICS/UMD	DSR-1210	Update/revisions for v02r07 (includes major algorithm revisions and software rejuvenation) CR-0054	10/01/2017
5	Hai-Tien Lee, CISESS/UMD	DSR-2063	Update for v03r00	04/28/2025

TABLE of CONTENTS

1. INTRODUCTION.....	7
1.1 Purpose	7
1.2 Definitions.....	7
1.3 Referencing this Document	8
1.4 Document Maintenance	8
2. OBSERVING SYSTEMS OVERVIEW.....	9
2.1 Products Generated.....	9
2.2 Instrument Characteristics	9
3. ALGORITHM DESCRIPTION.....	17
3.1 Algorithm Overview.....	17
3.2 Processing Outline	17
3.3 Algorithm Input	19
3.3.1 Primary Sensor Data	19
3.3.2 Ancillary Data.....	19
3.3.3 Derived Data	22
3.3.4 Forward Models.....	23
3.4 Theoretical Description.....	23
3.4.1 Physical and Mathematical Description.....	24
3.4.2 Data Merging Strategy.....	26
3.4.3 Numerical Strategy	26
3.4.4 Calculations.....	27
3.4.5 Look-Up Table Description.....	28
3.4.6 Parameterization	29
3.4.7 Algorithm Output.....	29
4. TEST DATASETS AND OUTPUTS.....	30
4.1 Test Input Datasets.....	30
4.2 Test Output Analysis.....	30
4.2.1 Reproducibility.....	30
4.2.2 Precision and Accuracy	31
4.2.3 Error Budget.....	35
5. PRACTICAL CONSIDERATIONS.....	36
5.1 Numerical Computation Considerations.....	36
5.2 Programming and Procedural Considerations.....	36
5.3 Quality Assessment and Diagnostics	36
5.4 Exception Handling.....	36
5.5 Algorithm Validation.....	37
5.6 Processing Environment and Resources	38
6. ASSUMPTIONS AND LIMITATIONS	39

6.1	Algorithm Performance	39
6.2	Sensor Performance.....	40
7.	FUTURE ENHANCEMENTS	41
7.1	Enhancement 1 – Reprocessing of IASI and CrIS OLR.....	41
7.2	Enhancement 2 – Metop-SG IASI-NG.....	41
7.3	Enhancement 3 – CrIS OLR Retrieval.....	41
7.4	Enhancement 4 – OLR Diurnal Model	41
8.	REFERENCES.....	42
	APPENDIX A. ACRONYMS AND ABBREVIATIONS.....	45
	APPENDIX B. IASI AND CRIS OLR RETRIEVAL ALGORITHMS.....	46
	APPENDIX C. HIRS OLR REGRESSION MODEL (V3.0) FOR DAILY OLR V2.0 AND MONTHLY OLR V3.0 CDR	49
	APPENDIX D. INTER-SATELLITE CALIBRATION FOR HIRS, IASI AND CRIS OLR RETRIEVALS 53	

LIST of FIGURES

Figure 1	Examples of the unapodized SDR radiances (black) and apodized radiances (red) for the three CrIS bands are shown, from top to bottom: LWIR, MWIR, and SWIR.....	15
Figure 2	Equator crossing times for the ascending orbit of the NOAA TIROS-N series POES, Metop and JPSS-series satellites.....	16
Figure 3	OLR CDR production system overview.....	18
Figure 4	OLR CDR production flow chart.....	19
Figure 5	TOA upward longwave radiation spectrum for standard mid-latitude summer case. The smooth curves are the Planck function evaluated at 200°K, 250°K and 294°K (surface temperature for this case), respectively for reference purpose.	24
Figure 6	Differences of Global mean OLR CDR between the Rejuvenated and the baseline version of the v02r07 code packages. (Rejuvenated version is labeled as “Pack5d”).....	31
Figure 7	Similar to Figure 6 but is for the standard deviation of the global monthly mean OLR differences.....	31
Figure 8.	The OLR differences between Daily OLR CDR v02R00 and the CERES EBAF Ed4.2 on the monthly basis: (a) mean OLR differences, and (b) standard deviation of the OLR differences, over	

the period of March 2000 to December 2023. Most areas in (a) are shown to have relative biases to within ± 2 Wm⁻², with standard deviations within 2 Wm⁻² in most areas.32

Figure 9 Mean, Std and RMS differences of the global mean OLR, Monthly OLR CDR v3.0 minus EBAF Ed4.2.....33

Figure 10 Mean, Std and RMS differences of the tropical mean OLR, Monthly OLR CDR v3.0 minus EBAF Ed4.2.....33

Figure 11 Comparison of OLR anomalies between the Monthly OLR CDR v3.0 (blue) and the CERES EBAF Ed4.2 (red) OLR products over the (a) global and (b) tropical 20S-20N domains. The differences of the OLR anomalies for global and tropical domains are shown in (c) and (d), respectively.....34

LIST of TABLES

Table 1 Versions of the OLR CDR product release, the corresponding software package, and the CATBD 8

Table 2 Description of instrument parameters for variant versions of HIRS instruments with an assumed satellite altitude of 833 km10

Table 3 Description of HIRS channel spectral locations and sensing properties. The channels that are used by OLR algorithm are shown. Note that the OLR retrieving channels for HIRS/3 and 4 are different from those of HIRS/2. There are seven channels that are used in the OLR retrieval. 11

Table 4 Description of HIRS instrument type and Level-1b data set coverage available for the OLR CDR production.....12

Table 5 Description of IASI instrument data set type and coverage available for the OLR CDR production.....13

Table 6 CrIS spectral resolution, frequency range, number of channels of the Unapodized spectrum and SDR product radiance spectra.....14

Table 7 Description of CrIS instrument data set type and coverage available for the OLR CDR production.....14

Table 8 HIRS/IASI/CrIS OLR intersatellite bias adjustments (Ed3d1), in unit Wm⁻². The Adjustment amount is to be subtracted from the OLR retrievals of the corresponding satellite.21

Table 9 Error sources and best estimated magnitude for OLR CDR production.....35

1. Introduction

1.1 Purpose

This document outlines the Monthly Outgoing Longwave Radiation (OLR) Climate Data Record (CDR) algorithm and software package. The HIRS multi-spectral OLR algorithm utilizes radiance observations from the HIRS instruments on TIROS-N and Metop series polar orbiters to estimate OLR accurately. The self-contained and highly portable software package plays a pivotal role in generating the OLR CDR. It encompasses all the necessary components and functionalities required for the production of Daily OLR CDR.

As an extension from the initially HIRS-based OLR CDR, the OLR CDR has been expanded to include consistent estimation of OLR using hyperspectral radiance observations from the Infrared Atmospheric Sounding Interferometer (IASI) on the Metop-series satellites and the Cross-Track Infrared Sounder (CrIS) on the JPSS-series satellites. This integration of HIRS, IASI, and CrIS OLR retrievals enables the generation of a continuous OLR time series, as gridded global maps, from 1979 to the present, and onward.

The explanations of the algorithm and the software package provide a guide to the understanding of algorithm theoretical basis and performance, as well the product generation procedures.

1.2 Definitions

Following is a summary of the symbols used to define the algorithm.

Spectral and directional parameters:

λ = wavelength (μm)

ν = wavenumber (cm^{-1})

θ = view zenith angle or local zenith angle (degree)

ϕ = relative azimuth angle (degree)

$I_v^\uparrow(z_t; \theta, \phi)$ = upward specific intensity at height z ($\text{Wm}^{-2} \text{sr}^{-1} (\text{cm}^{-1})^{-1}$)

$\Phi_i(\nu)$ = normalized spectral response function for the i^{th} channel (unit-less)

$N_i(\theta, \phi)$ = TOA radiance observed from satellite for the i^{th} channel ($\text{Wm}^{-2} \text{sr}^{-1} (\text{cm}^{-1})^{-1}$)

$N_{\Delta\nu}(\theta, \phi)$ = TOA radiance integrated over wavenumber interval $\Delta\nu$ ($\text{Wm}^{-2} \text{sr}^{-1}$)

$F^\uparrow(z_t; \theta, \phi)$ = upward radiant flux intensity at height z ($\text{Wm}^{-2} \text{sr}^{-1}$)

$F_v^\uparrow(z)$ = upward spectral flux at height z ($\text{Wm}^{-2} (\text{cm}^{-1})^{-1}$)

$F^\uparrow(z)$ = upward flux (cf. radiant flux density, or irradiance) at height z (Wm^{-2})

$B_\nu(T)$ = Planck function evaluated at wavenumber ν at temperature T ($\text{Wm}^{-2} \text{sr}^{-1} (\text{cm}^{-1})^{-1}$)

C_1 = First Planck function coefficient ($\text{Wm}^{-2} \text{sr}^{-1} (\text{cm}^{-1})^{-1} (\text{cm}^{-1})^{-3}$)

C_2 = Second Planck function coefficient ($(\text{cm}^{-1})^{-1}$ Kelvin)

Atmospheric parameters:

$$\tau_v(z; \theta) = \text{optical depth (unit-less)}$$

1.3 Referencing this Document

This document should be referenced as follows:

Outgoing Longwave Radiation - Monthly - Climate Algorithm Theoretical Basis Document, NOAA Climate Data Record Program CDRP-ATBD-0097 Rev. 5 (2025), available at <http://www.ncei.noaa.gov/cdr/operationalcdrs.html>

1.4 Document Maintenance

Table 1 defines the versions of the OLR CDR product release, the corresponding software package, and the CATBD. The Production software package is maintained at NCEI Subversion version control system.

Table 1 Versions of the OLR CDR product release, the corresponding software package, and the CATBD

Release Date	Product Version	Software Version	CATBD Version	Subversion Branch	Remarks
2011-09-01	V02R02	V02R02	v1.0		Initial Release
2017-10-01	V02R07	V02R07	v4.0		Upgrade revision
2023-11-01	V02R07*	V02R08	Technical Note for IASI/CrIS Data Extension 2007-present for Monthly OLR CDR		Interim update for new additions of IASI and CrIS OLR retrievals. Re-released as "v02r07 reprocessed" with data reprocessed from 2007-present
2025-05-01	V03R00	V03R00	v5.0		Major upgrade

2. Observing Systems Overview

2.1 Products Generated

The product generated is the monthly mean OLR time series in 2.5°x2.5° equal-angle gridded global maps spanning from January 1979 to the present (and continues on). The OLR is estimated directly from the radiance observations made by HIRS, IASI and CrIS, for all sky conditions. The HIRS instruments are flown onboard the NOAA TIROS-N series and Eumetsat Metop-A/B operational polar-orbiting satellites. The IASI instruments are flown onboard the Metop-series satellites (A, B, C), and the CrIS instruments are flown onboard the JPSS-series satellites (S-NPP, J01, J02).

OLR is one of the three components that determine the top of the atmosphere (TOA) earth radiation budget (ERB). OLR has been extensively used in the investigations of the cloud/water vapor/radiative interaction processes, climate variability, climate change monitoring, numerical model evaluation and diagnostics, and applications in tropical dynamics and precipitation, etc. OLR is identified as one of the “Essential Climate Variables” in WMO Global Climate Observing System (GCOS).

2.2 Instrument Characteristics

A. HIRS

HIRS is one of the three sounding instruments that constitute the TIROS Operational Vertical Sounder (TOVS, and later becomes Advanced TOVS, ATOVS) system onboard the NOAA TIROS-N series and Eumetsat Metop-A/B satellites. The detailed description of HIRS instrument characteristics, Level-1b data format, the TOVS system, and the system configurations for the NOAA TIROS-N series polar orbiters can be found in the NOAA Polar Orbiter Data (POD) User's Guide (1998 version) and NOAA KLM User's Guide (2009 version).

There are some relatively minor variations in HIRS instrument design. **Table 2** lists the HIRS instrument parameters for the variant versions (cf. NOAA POD User's Guide Table 4.0-1; NOAA KLM User's Guide Section 3.2.2 and Appendix J). It's noteworthy to point out that the onboard warm target calibration reference has been changed from two blackbodies in HIRS/2 and 2I to one blackbody in HIRS/3 and 4. The HIRS/4 FOV resolution is enhanced to 10 km, which is about a two-fold improvement over the earlier HIRS versions.

Table 2 Description of instrument parameters for variant versions of HIRS instruments with an assumed satellite altitude of 833 km

Parameters	HIRS/2	HIRS/2I	HIRS/3	HIRS/4
Calibration	Two Stable blackbodies and space background	Two Stable blackbodies and space background	One Stable blackbody (290K) and space background	One Stable blackbody (286K) and space background
Cross-track scan angle (degrees from nadir)	± 49.5	± 49.5	± 49.5	± 49.5
Scan time (seconds)	6.4	6.4	6.4	6.4
Number of steps	56	56	56	56
Angular FOV (degrees)	1.22	1.40	1.40 (Ch1-12) 1.3 (Ch13-19)	0.69
Step angle (degrees)	1.8	1.8	1.8	1.8
Step time (seconds)	0.1	0.1	0.1	0.1
Ground IFOV at nadir (km diameter)	17.4	20.4	20.3 (Ch1-12) 18.9 (Ch13-19)	10
Ground IFOV at end of scan	58.5 km cross-track x 29.9 km along-track	68.3 km cross-track x 34.8 km along-track	68.3 km cross-track x 34.8 km along-track	34.2 km cross-track x 17.4 km along-track
Distance between IFOV centers (km along-track)	42.0	42.0	42	42
Swath width	± 1120 km	± 1124 km	± 1124 km	± 1107 km
Data precision (bits)	13	13	13	13

HIRS consists of nineteen infrared channels (channels 1-19) and one visible channel (channel 20). **Table 3** lists the central wavenumbers and the sensing properties for the HIRS/2 on NOAA-9 as an example, with the channels used in HIRS OLR algorithm indicated. Specifications for HIRS/3 and 4 are available on NOAA KLM User's Guide.

Table 3 Description of HIRS channel spectral locations and sensing properties. The channels that are used by OLR algorithm are shown. Note that the OLR retrieving channels for HIRS/3 and 4 are different from those of HIRS/2. There are seven channels that are used in the OLR retrieval.

Channel	Central wavenumber (cm ⁻¹)	Used in HIRS/2 OLR Algorithm	Sensing Properties
1	667.67		15 μm CO ₂ band
2	679.84		15 μm CO ₂ band
3	691.46	✓	15 μm CO ₂ band
4	703.37		15 μm CO ₂ band
5	717.16	✓	15 μm CO ₂ band
6	732.64		15 μm CO ₂ band
7	749.48	✓	15 μm CO ₂ band
8	898.53	✓	Window
9	1031.61	✓	Ozone
10	1224.74		Water Vapor
11	1365.12	✓	Water Vapor
12	1483.24	✓	Water Vapor
13	2189.97		4.3 μm CO ₂ band
14	2209.18		4.3 μm CO ₂ band
15	2243.14		4.3 μm CO ₂ band
16	2276.46		4.3 μm CO ₂ band
17	2359.05		4.3 μm CO ₂ band
18	2518.14		Window
19	2667.80		Window
20	14549.27		Visible Window

Table 4 describes the HIRS instrument types and the availability of HIRS Level-1B data. The near real-time instrument health condition is available at NESDIS POES Status Monitoring website (<http://www.oso.noaa.gov/poesstatus/> as of July 18, 2011). The satellite ID is the code name for these polar orbiters that will be referred in the OLR CDR production package and in this document henceforth.

Errata: The Note 7 of Table J.1 on KLM User's Guide Appendix J states that "HIRS/2I was flown on NOAA-14 only". This statement is incorrect. HIRS/2I instruments were flown on both NOAA-11 and 14.

Table 4 Description of HIRS instrument type and Level-1b data set coverage available for the OLR CDR production.

Satellite	Satellite ID	Data coverage	Instrument Type
TIROS-N (TN)	N05	1978 d294 – 1980 d054	HIRS/2
NOAA-6 (NA)	N06	1979 d181 – 1983 d064 1985 d098 – 1985 d181 1985 d290 – 1986 d319	HIRS/2
NOAA-7 (NC)	N07	1981 d236 – 1985 d032	HIRS/2
NOAA-8 (NE)	N08	1983 d123 – 1984 d163 1985 d182 – 1985 d287	HIRS/2
NOAA-9 (NF)	N09	1984 d348 – 1988 d312	HIRS/2
NOAA-10 (NG)	N10	1986 d329 – 1991 d259	HIRS/2
NOAA-11 (NH)	N11	1988 d313 – 1995 d100 1997 d196 – 2000 d117	HIRS/2I
NOAA-12 (ND)	N12	1991 d259 – 1998 d348	HIRS/2
NOAA-14 (NJ)	N14	1995 d001 – 2006 d283	HIRS/2I
NOAA-15 (NK)	N15	1998 d299 – 2009 d120	HIRS/3
NOAA-16 (NL)	N16	2001 d001 – 2014 d165	HIRS/3
NOAA-17 (NM)	N17	2002 d191 – 2013 d099	HIRS/3
NOAA-18 (NN)	N18	2005 d156 – present	HIRS/4
NOAA-19 (NP)	N19	2009 d153 – present	HIRS/4
Metop-A	M02	2006 d325 – 2021 d304	HIRS/4
Metop-B	M01	2013 d015 – 2023 d076	HIRS/4

B. IASI

The IASI instrument is an infrared Fourier Transform Spectrometer, with cross-track scanning pattern, measuring the upwelling infrared radiances at very high spectral resolution. It is currently flying on Metop-1 and Metop-3 satellites and will also fly on the subsequent Metop satellites. The Metop-series polar satellites are in sun-synchronous orbits with nominal Equator Crossing Time of 2130 and 0930, for ascending and descending orbits, respectively.

IASI Level-1C (L1C) is apodized Level 1b to obtain a nominal Instrument Spectral Response Function. Eumetsat performs and provides the L1C data sets (refer to the IASI Products webpage https://iasi.cnes.fr/en/IASI/A_products.htm).

The IASI interferometer field of view is square, seen under an angle of $3.33^\circ \times 3.33^\circ$ (~15km). Information matrix of 2×2 circular pixels are seen under an angle of 1.25° . The overall swath is $\pm 48.3^\circ$ with respect to the nadir direction, corresponding to 30 mirror positions. (cf.

https://www.esa.int/Applications/Observing_the_Earth/Meteorological_missions/MetOp/About_IASI)

The IASI L1C data covers the spectral range from 645 to 2760 cm^{-1} continuously, at a resolution of 0.5 cm^{-1} , sampled at every 0.25 cm^{-1} . The IASI L1C data files are grouped by ~3 minutes granuals, at ~60MB per file, or, about 28GB per day. The IASI L1C product format is described by the "IASI Level 1 Product Format Specification (Eumetsat EUM.EPS.SYS.SPE.990003)" document. More descriptions for IASI L1C data can be found at <https://navigator.eumetsat.int/product/EO:EUM:DAT:METOP:IASIL1C-ALL>.

The IASI L1C data set availability is described in **Table 5**.

Table 5 Description of IASI instrument data set type and coverage available for the OLR CDR production.

Satellite	Satellite ID	Data coverage	Data Type
Metop-A	M02	2007.05.21 – 2021.10.15	L1C
Metop-B	M01	2013.08.01 – present	L1C
Metop-C	M03	2019.07.06 – present	L1C

C. CrIS

The CrIS instrument is an infrared Fourier Transform Spectrometer, with cross-track scanning pattern, measuring the upwelling infrared radiances at very high spectral resolution. It has been flown on Sumi-NPP satellite and are currently operational on NOAA-20/21 satellites, and will be flown on the JPSS-3, and 4 satellites. The JPSS-series polar satellites have a nominal Equator Crossing Time of 0130/1330.

CrIS spectral coverage includes three bands: SWIR: 3.92-4.64 micron; MWIR: 5.71-8.26 micron; LWIR: 9.14-15.38 micron. For the nominal model, Normal Spectral Resolution (NSR), there are 1305 spectral channels, with spectral resolution at 0.625, 1.25, and 2.5 cm^{-1} for the LWIR, MWIR, SWIR bands, respectively. While for the Full Spectral Resolution (FSR), there are 2211 spectral channels, at 0.625 cm^{-1} resolution for all three bands.

One CrIS cross-track scan contains 30 Field of Regards (FOR), while each FOR is consist of 9 (3x3) FOVs.

Table 6 shows the CrIS spectral resolution, frequency range, number of channels of the Unapodized spectrum and SDR product radiance spectra. (Taken from Table 4 of Cross Track Infrared Sounder (CrIS) Sensor Data Record (SDR) User's Guide Version 1.1 (April 2018)). Examples of the unapodized and SDR radiances for the three CrIS bands are shown in **Figure 1**. **Table 7** describes the CrIS SDR data set availability.

Table 6 CrIS spectral resolution, frequency range, number of channels of the Unapodized spectrum and SDR product radiance spectra.

Band/Spectral Resolution	Resolution (cm^{-1})	Unapodized Spectrum		SDR Specification	
		Frequency Range (cm^{-1})	Number of Channels	Spectral Range (cm^{-1})	Number of Channels
LWIR	0.625	648.75 – 1096.25	717	650-1095	713
MWIR NSR	1.25	1207.5 – 1752.5	437	1210-1750	433
MWIR FSR	0.625	1208.75 – 1751.25	869	1210-1750	865
SWIR NSR	2.5	2150 - 2555	163	2155-2550	159
SWIR FSR	0.625	2153.75 – 2551.25	637	2155-2550	633

Table 7 Description of CrIS instrument data set type and coverage available for the OLR CDR production.

Satellite	Satellite ID	Data coverage	Data Type
S-NPP	NPP	2012.04.01 – 2021.05.21	SDR - NSR/FSR
JPSS-1 (J01)	NOAA20	2017.03.08 – present	SDR - FSR
JPSS-2 (J02)	NOAA21	2023.04.12 – present	SDR - FSR

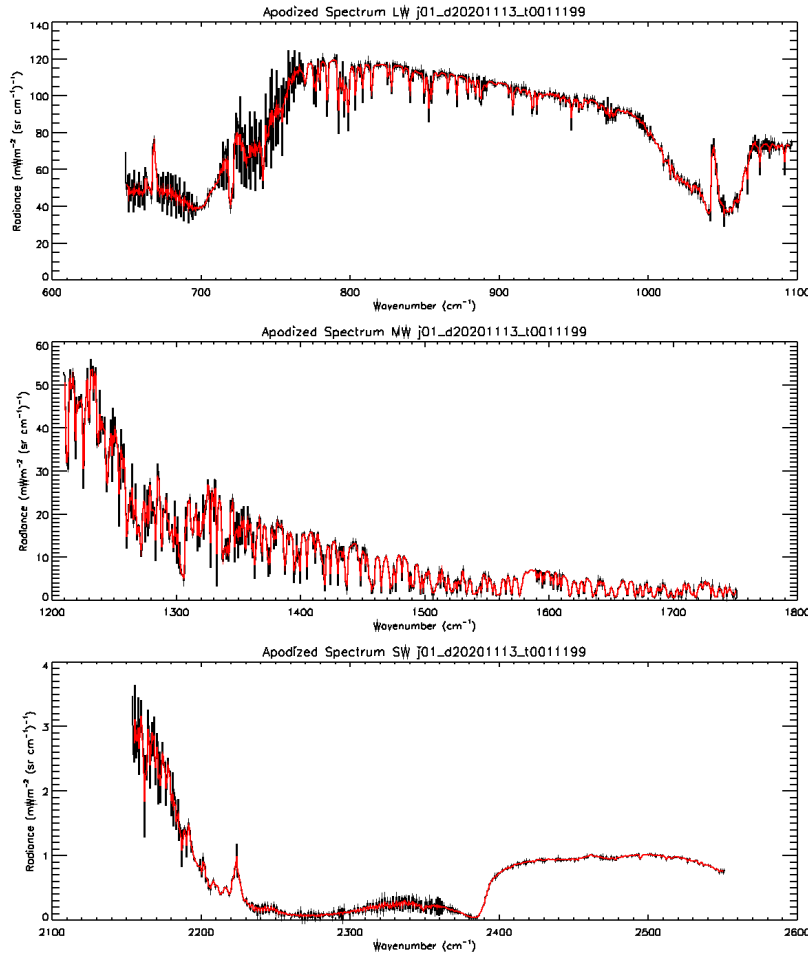


Figure 1 Examples of the unapodized SDR radiances (black) and apodized radiances (red) for the three CrIS bands are shown, from top to bottom: LWIR, MWIR, and SWIR.

NOAA POES were historically configured to fly with one morning and one afternoon satellites, nominally at 7:30 and 2:30 equator crossing time, respectively. The polar-orbiter configuration was changed since NOAA-17, which was moved to the late morning 10:30 orbit. Since they are all in processing orbits, their equator crossing times change slowly corresponding to the orbital drifts. **Figure 2** describes the equator crossing times of the NOAA POES TIROS-N, Metop and JPSS-series satellites in their course of operation, for the ascending branch of the orbits. Note that the Metop and JPSS satellites are in controlled orbits, with near constant equator crossing time of 21:30 and 01:30 ascending orbits, respectively.

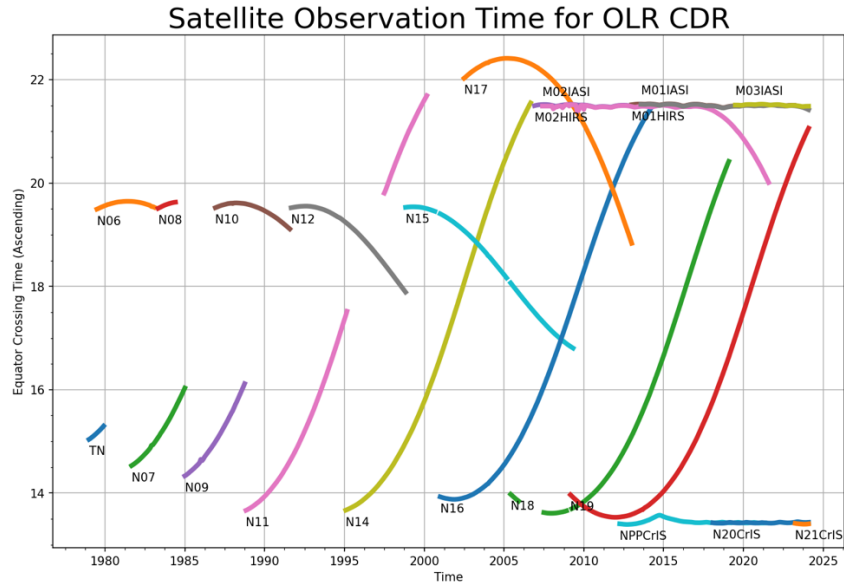


Figure 2 Equator crossing times for the ascending orbit of the NOAA TIROS-N series POES, Metop and JPSS-series satellites.

3. Algorithm Description

3.1 Algorithm Overview

The multi-spectral OLR estimation method was developed by Ellingson et al. (1989) that use narrowband radiance observations from the High-resolution Infrared Sounder (HIRS) to estimate TOA total longwave flux. Vigorous validation efforts were performed for the HIRS OLR estimation technique against broadband observations derived from the Earth Radiation Budget Experiment (ERBE) and the Clouds and the Earth's Radiant Energy System (CERES) (see Ellingson et al., 1994; Lee et al., 2007). The multi-spectral OLR estimation technique has been adapted successfully to the GOES- Sounder (Ba et al., 2003) and GOES-Imager instruments (Lee et al., 2004). These studies have shown that this OLR estimation algorithm can reliably achieve with an accuracy of about 4 to 8 Wm^{-2} for various instrument type, with biases (precision) that are within the respective radiometric accuracy of the reference instruments. The HIRS OLR algorithm has been implemented to generate the NESDIS operational HIRS OLR product since September 1998, and the GOES Imager OLR is implemented as part of the operational GOES Surface and Insolation Product (GSIP). A variant of this method has been developed and implemented for the upcoming GOES-R Advanced Baseline Imager instrument (Lee et al., 2010).

3.2 Processing Outline

The OLR CDR algorithm derives monthly mean OLR using all available HIRS, IASI, and CrIS radiance observations from the operational polar-orbiting satellites, including the TIROS-N series, Metop-series and JPSS-series satellites. The primary input is the HIRS Level-1b, IASI Level-1C and CrIS SDR data files. This algorithm performs HIRS radiance calibration independently from the operational calibration methods such that the radiance calibration is consistent throughout the OLR time series. **Figure 3** provides the overview for the OLR CDR production system. **Figure 4** is the OLR CDR production flow chart that explains the execution sequences and input/output relationships.

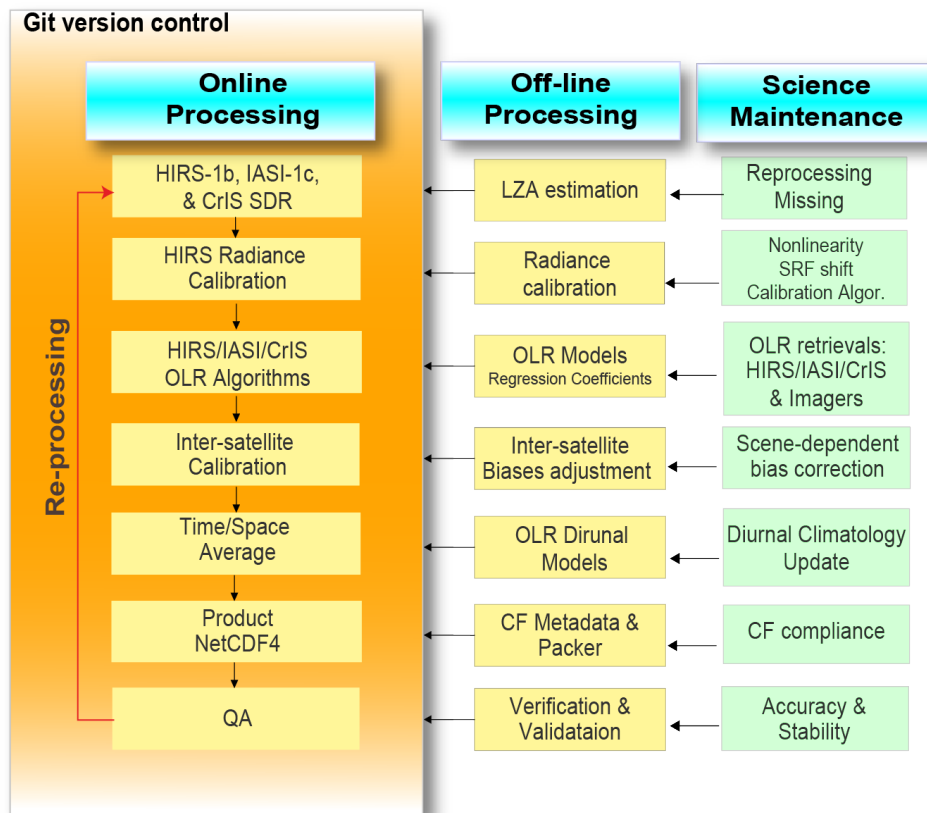


Figure 3 OLR CDR production system overview.

**Main Processing Sections of the
Outgoing Longwave Radiation – Monthly CDR (01B-06)
Operational Monthly Execution Top View Flow Chart**

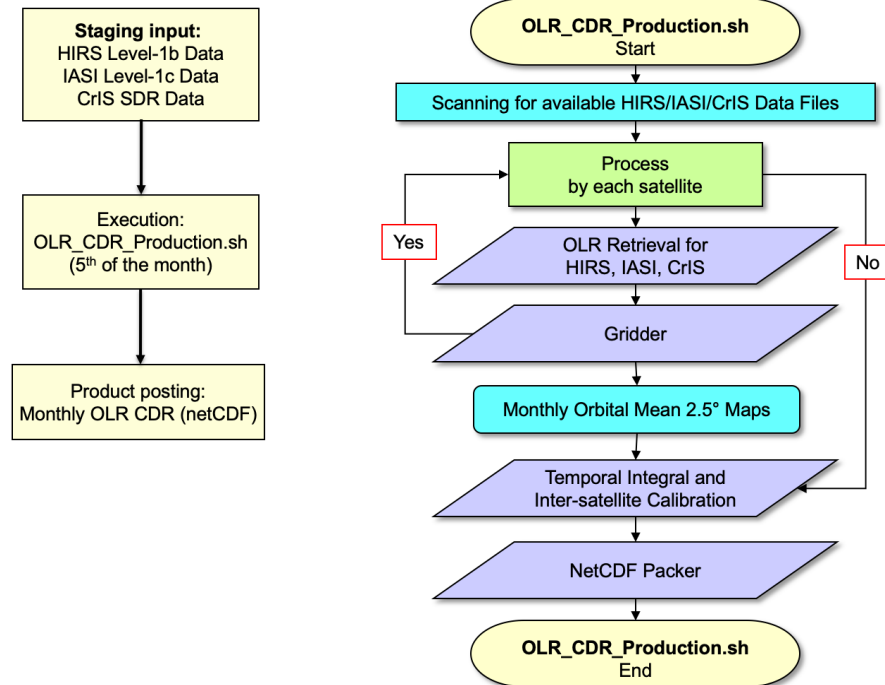


Figure 4 OLR CDR production flow chart.

3.3 Algorithm Input

3.3.1 Primary Sensor Data

The primary input data for the OLR CDR algorithm include the HIRS Level-1B, IASI Level-1C, and CrIS SDR data. The HIRS Level-1B data available from NCEI CLASS, and is used to determine the HIRS radiances, which is used in HIRS OLR retrieval. The IASI Level-1C and CrIS SDR data, also available from NCEI CLASS are used for IASI and CrIS OLR retrieval, respectively.

The OLR CDR production package includes a HIRS radiance calibration component that consistently derives HIRS radiances from the HIRS Level-1B data. The calibration module handles the variation in the format of HIRS Level-1b accordingly.

3.3.2 Ancillary Data

There are five groups of ancillary data (namely, the static data) that are required for the OLR CDR production: a) the OLR regression coefficients, b) the calibration

prediction coefficients; c) OLR inter-satellite bias adjustments; d) OLR diurnal model coefficients; and e) Time stamp template. These static data in (a)-(c) are satellite-specific.

a) OLR Regression Coefficients

The coefficients for the HIRS OLR v3.0 regression model is derived from a set of IASI-simulated HIRS radiances and fluxes (see Appendix C for details). The regression coefficients included in this package has a code name "v3c6".

Format	ASCII tabulated, 10 columns x 6500 lines
Version	V3c6 (based on IASI-simulations)
Size	910KB each; Total 15 MB for 16 files (TIROS-N, N06, ..., N18, N19, M02, M01).
Location	Data_static/OLR_coef_v3c6/coef_\${satid}_305_a19.asc (see Scripts/OLR_retrieval.sh)
Access	Local
Reference	Code package

The coefficients for the IASI OLR regression model are derived from a set of IASI-simulated radiances and fluxes (see Appendix B for details).

Format	IDL Save file, dimensions: OLR_COEF_TABLE 7x305x650; PRED_TABLE 3x305
Version	J00
Size	5.6 MB
Location	[IASI_package] Data_static/IASI_OLR_coef_J00.save
Access	Local
Reference	Code package get_iasi_olr_coef.pro

The coefficients for the CrIS OLR regression model are derived from a set of IASI-simulated radiances and fluxes (see Appendix B for details).

Format	IDL Save file, dimensions: OLR_COEF_TABLE 7x305x650; PRED_TABLE 3x305
Version	J00
Size	11.1 MB
Location	[CrIS_package] Data_static/CrIS_OLR_coef_J00.save.save
Access	Local
Reference	Code package get_cris_olr_coef.pro

b) Calibration Prediction Coefficients

There are sets of coefficients that are required by the McMillin radiance calibration method (NOAA POD Users Guide, 1998). They are also satellite specific. The

generation and updates of these coefficients are discussed in Lee et al. (2007) and the technical report “McMillin HIRS Radiance Calibration Method”.

Format	ASCII
Version	Ver.1: N05 – N12 Ver.2: N14 Ver.3: N15 – N21 (Refer /Utility/define_pred_version.sh)
Size	25 KB per satellite; Total 375 KB.
Location	/Data_static/cali_data/\${satid} (refer /Scripts/OLR_retrieval.sh)
Access	Local
Reference	/Documentations/Publications/Lee 2007 HIRS OLR CDR.pdf /Documentations/Tech_Report/McMillin HIRS Radiance Calibration Method.pdf

c) OLR Intersatellite Bias Adjustments

The methodology for deriving the bias adjustments are described in Lee et al. (2007) with the update to reflect the v2.7 OLR retrievals. For the Daily OLR CDR v2.0 upgrade, the methodology has been revised and the inter-satellite adjustments are determined with the instantaneous FOV OLR data from the HIRS v3.0 OLR retrievals, and IASI/CrIS OLR retrievals. (see Table 8 and Appendix D for details and).

Format	ASCII
Version	V3d1
Size	4 KB
Location	Data_static/Intersat_Adjustment_Ed3d1.dat (refer /Scripts/OLR_daily_integral.sh)
Access	Local
Reference	Table 5

Table 8 HIRS/IASI/CrIS OLR intersatellite bias adjustments (Ed3d1), in unit Wm^{-2} . The Adjustment amount is to be subtracted from the OLR retrievals of the corresponding satellite.

Satellite ID	Ed3d1	Satellite ID	Ed3d1
TIROS-N HIRS	0.028	N17 HIRS	-0.177
N06 HIRS	-0.739	N18 HIRS	-0.333
N07 HIRS	-0.138	N19 HIRS	-0.206
N08 HIRS	-0.216	M02 HIRS	-0.045
N09 HIRS	-0.122	M01 HIRS	-0.017
N10 HIRS	-0.004	M02 IASI	0.000
N11 HIRS	-0.049	M01 IASI	-0.035
N12 HIRS	-0.198	M03 IASI	-0.193
N14 HIRS	-0.341	S-NPP CrIS	1.387

A controlled copy of this document is maintained in the CDR Program Library.
Approved for public release. Distribution is unlimited.

N15 HIRS	0.263	J01/N20 CrIS	1.395
N16 HIRS	0.043	J02/N21 CrIS	1.265

d) OLR Diurnal Model Coefficients

The construction of the climatological OLR diurnal models is discussed in details in Lee et al. (2007). These models described the climatological OLR diurnal variations for each month at each of the 2.5°x2.5° region on the monthly mean basis. They are used in the OLR monthly mean temporal integral calculations.

Format	IEEE Binary (direct access, unformatted, record length=4*144*72*12*4 Bytes) (refer /Codes/Temporal/OLR_monthly_integral.f90)
Version	Ver.1
Size	2 MB
Location	Data_static/coef_diurnal_model.dat (refer /Scripts/OLR_monthly_integral.sh)
Access	Local
Reference	Documentations/Publications/Lee 2007 HIRS OLR CDR.pdf

e) Time Stamp Template

The time stamp template file contains time markers as the increments in days (real number) since Jan 1. 1979 00:00:00Z. These predefined time markers include the time at the exact middle, and the beginning and the ending bounds for each month.

Format	ASCII (refer /Codes/Packer/OLR_CDR_nc4_batch.f90)
Version	Ver.1
Size	12 KB
Location	Data_static/Time_template_720.dat
Access	Local
Reference	Documentations/Publications/Lee 2007 HIRS OLR CDR.pdf

3.3.3 Derived Data

Not applicable.

Remark: The radiance calibration module takes the HIRS Level-1B data as the input and derives the HIRS radiance. The radiance is then passed directly to the OLR regression model without being written to an intermediate data file.

3.3.4 Forward Models

Not applicable.

3.4 Theoretical Description

The HIRS CDR OLR production is a sequential processing. The sequence and the relevant processing are described here. See “OLR_CDR_Production.sh” script file for more details.

a. Radiance Calibration

The OLR CDR production starts with the derivation of the radiance from the HIRS Level-1B data by the radiance calibration module. The radiance calibration is performed consistently throughout the HIRS OLR time series with the McMillin radiance calibration method.

The IASI and CrIS radiance calibration is defined and performed by the algorithms defined in the operational or reprocessing processing. Their hyperspectral radiance data is used as is.

b. OLR Retrieval (HIRS, IASI, CrIS)

The multi-spectral OLR estimation technique is applied here. The OLR is retrieved at each HIRS FOV with the given radiances and local zenith angles.

The IASI and CrIS OLR retrieval algorithm is explained in Appendix B.

The new, v3.0 HIRS OLR retrieval model is explained in Appendix C.

c. Intersatellite Calibration

Inter-satellite calibration between the HIRS, IASI and CrIS OLR retrievals is performed by applying the pre-determined bias adjustments relative to the reference Metop-A (M02) IASI OLR retrievals. The determination of the inter-satellite calibration adjustments can be found in Appendix D.

d. Gridding of OLR Monthly Orbital Maps

For each satellite, each month, the OLR retrievals (at FOV) are gridded into two 2.5°x2.5° equal-angle maps, consisting of observations from the ascending and descending orbits, respectively.

e. Temporal Integration for Monthly Mean and Intersatellite Bias Adjustment

The OLR monthly mean is derived from the gridded OLR monthly orbital maps of all the contributing satellites. The monthly orbital maps can be considered as the monthly mean OLR at local times.

Inter-satellite calibration between the HIRS, IASI and CrIS OLR retrievals is performed by applying the pre-determined bias adjustments relative to the reference

Metop-A (M02) IASI OLR retrievals. The determination of the inter-satellite calibration adjustments can be found in Appendix D. Then the temporal integral is independently performed for each of the 144x72 grids.

The diurnal variation envelopes prescribed by the OLR diurnal models is constrained by the observed OLR retrievals obtained at different observing local times. The OLR monthly mean value is then determined as the integral of the constrained envelop curve over the 24 hours period.

f. NetCDF packing

The last step is NetCDF packing for the release product file. The OLR CDR product is a single NetCDF file that contains the entire time series starting on January 1979. The newly retrieved monthly mean OLR data will be added to the existing time series and a new NetCDF product file will be generated for release.

3.4.1 Physical and Mathematical Description

The specific intensity I_ν of upward longwave radiation at the top of the atmosphere z_t at local zenith angle θ and azimuth angle ϕ , can be expressed as:

$$I_\nu^\uparrow(z_t; \theta, \phi) = \varepsilon_\nu^* B_\nu^*(0) T_\nu^*(z_t, 0; \theta, \phi) + \int_0^{z_t} B_\nu^*(z') \frac{\partial T_\nu(z_t, z'; \theta, \phi)}{\partial z'} dz' \quad (1)$$

where T_ν is the monochromatic atmospheric transmittance, T_ν denotes the surface emissivity, $B_\nu(z')$ is the Planck function evaluated at wave number ν with the temperature at level z' . The black surface is assumed here.

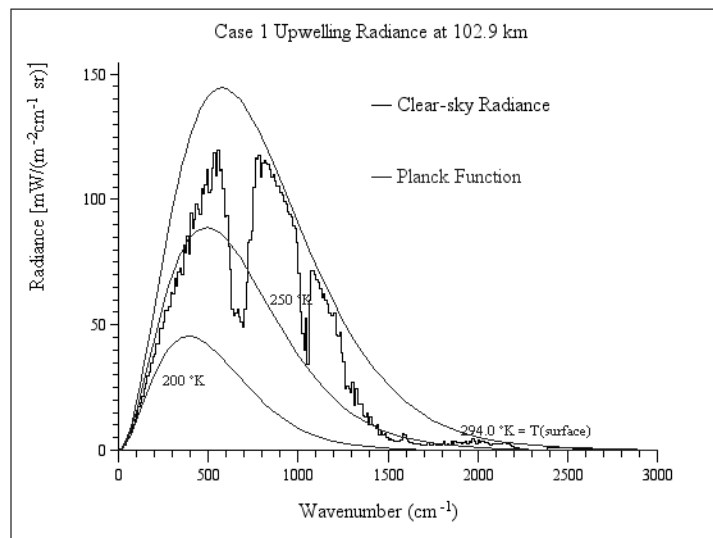


Figure 5 TOA upward longwave radiation spectrum for standard mid-latitude summer case. The smooth curves are the Planck function evaluated at 200°K, 250°K and 294°K (surface temperature for this case), respectively for reference purpose.

The outgoing longwave radiation (*OLR*), whose example spectrum is shown in **Figure 5**, is the radiative flux through a unit area at the top of the atmosphere that is related to the specific intensity by integrating over wavenumbers (ν) and over hemispheric solid angles (θ and ϕ):

$$OLR = \int_0^{2\pi} \int_0^{\pi/2} \int_0^{\infty} I_{\nu}^{\uparrow}(z_i; \theta, \phi) \cos \theta \, d\nu \sin \theta \, d\theta \, d\phi \quad (2)$$

Ellingson et al. (1989) formulated the multi-spectral OLR algorithm that expresses the OLR as a linear combination of the radiances (N_i) of selected channels, observed at a local zenith angle θ :

$$OLR = a_0(\theta) + \sum_i a_i(\theta) \cdot N_i(\theta) \quad (3)$$

The satellite-observed narrowband radiance N_i of channel i can be described by the convolution of the TOA specific intensity with the respected spectral response function Φ_i

$$N_i(\theta, \phi) = \int_{\nu_i} I_{\nu}^{\uparrow}(z_i; \theta, \phi) \cdot \Phi_i(\nu) \, d\nu \quad (4)$$

The azimuth angle dependence in the radiance is removed when axial-symmetry is assumed. The bounds of the wavenumber integral for OLR are 0 to 3000 cm^{-1} .

The new v2.7 HIRS OLR algorithm developed for the daily OLR CDR is revised to include non-linear radiance terms in the predictors, generalized in this form:

$$OLR = a_0(\theta) + \sum_i a_i(\theta) \cdot N_i^p(\theta) \quad (5)$$

where p denotes the power that corresponding channel radiance is being raised.

The v2.7 HIRS OLR model now consists of the radiance predictors from HIRS channels: 3, 7, 8, 11, 82, 110.5, 120.5, with the exponents indicating the raised powers, such as this:

$$OLR = a_0(\theta) + a_1(\theta) \cdot N_3(\theta) + a_2(\theta) \cdot N_7(\theta) + a_3(\theta) \cdot N_8(\theta) + a_4(\theta) \cdot N_{11}(\theta) \\ + a_5(\theta) \cdot N_8^2(\theta) + a_6(\theta) \cdot N_{11}^{0.5}(\theta) + a_7(\theta) \cdot N_{12}^{0.5}(\theta) \quad (6)$$

The OLR regression coefficients are determined from a set of 3717 radiation simulations by the Warner-Ellingson radiative transfer model (Warner and Ellingson, 2000) with Phillips soundings (termed m2s3 simulation method).

For Monthly OLR CDR v3.0 upgrade, the HIRS OLR model is slightly modified as in Eq. 7, with “m2s4” simulation database. See Appendix E for details.

$$OLR = a_0 + a_1N_3 + a_2N_7^{0.1} + a_3N_8 + a_4N_8^{0.5} + a_5N_{11} + a_6N_{11}^{0.5} + a_7N_{12}^{0.5} + a_8N_9 + a_9N_5 \quad (7)$$

3.4.2 Data Merging Strategy

The OLR CDR production uses multi-platforms observations that require critical data merging techniques to achieve consistency and continuity. Special cares are needed in OLR retrieval and temporal integration aspects.

- OLR retrieval

Obtaining consistent OLR retrievals from all satellites is achieved through two controlling factors: 1) consistent OLR regression models; 2) inter-satellite calibration.

The coefficients for OLR regression models are satellite/instrument specific. Since the coefficients are derived from a common set of simulations, the OLR regression models for different satellites and instruments would have consistent error characteristics, if the instruments are not changed. However, due to the variations in HIRS/2/2I/3, and 4, there are necessary changes in the OLR regression model formulation, which could result in inconsistencies in their regression error characteristics. This in turn will reduce the robustness of the inter-satellite calibration results.

There are other factors that can affect the accuracy of the OLR retrievals but not yet fully resolvable now, e.g., consideration of sensor non-linear response and uncertainties in spectral response functions. The current approach is to remove the bulk intersatellite OLR biases by directly comparing OLR retrievals between two satellites with collocated observations. This is a first order end-to-end correction on all the possible errors for the OLR retrievals from radiance calibration to the OLR model application.

- Temporal Integral

Polar orbiters have low temporal sampling rate – twice a day for a given location from each satellite. Although composite observations can be obtained from multiple polar orbiters, the orbital drift effects can alias into artifacts or spurious trends for the time series if temporal integral is not performed carefully. As an approximation, the OLR CDR uses the climatological OLR diurnal models to reduce the temporal integral errors related to orbital drifts. A better accuracy can be obtained when using OLR estimated from geostationary satellites. And this is for future improvement.

3.4.3 Numerical Strategy

Missing Value and Weaver Subroutine

The monthly mean OLR map could have missing values if the temporal integral performed at certain grid boxes failed, possibly due to insufficient OLR retrieval data. (Note that this is extremely rare if there are two or more satellites in each month.) Approximations

for such grids will be made with the Cressman interpolation (Cressman, 1959) by the Weaver subroutine.

3.4.4 Calculations

The OLR CDR Production includes the following steps:

- a) Compile.sh – clean compilation of all Fortran programs
- b) OLR_CDR_Production.sh - OLR CDR Production driver script
- c) OLR_retrieval.sh – HIRS radiance calibration and HIRS OLR retrieval

Note that the IASI and CrIS OLR retrieval are performed respectively in their own packages

- d) OLR_gridder.sh – Gridding of orbital maps
- e) OLR_monthly_integral.sh – Intersatellite bias adjustment and monthly mean temporal integral
- f) OLR_packer_batch.sh – Pack into NetCDF-4 product file

a) Compile.sh

- Compilation of all Fortran programs used in OLR CDR Production.

b) OLR_CDR_Production.sh

- Main driving script for OLR CDR production.
- In automated mode, it is to be executed once a month, presumed to be on the 5th day of a month.
- It can also be invoked with an argument of <yyyymm> to specify the month to be processed.

c) OLR_retrieval.sh

- Perform HIRS radiance calibration
- Retrieve OLR at each HIRS field of view (FOV)

d) OLR_gridder.sh

- Create OLR orbital maps for ascending and descending node respectively at 2.5°x2.5° equal-angle grid.

e) OLR_monthly_integral.sh

- Giving the monthly orbital mean maps from the available satellites, perform monthly mean integral constrained with OLR diurnal models.
- Integral is constrained with the climatological OLR diurnal models (monthly, 2.5°x2.5° in ECT time stamp).

f) OLR_packer_batch.sh

- Pack OLR CDR data into a NetCDF4 data file, including the previously derived months and the newly derived OLR monthly mean data stored in Work/OLR_CDR/archive_ascii/.

3.4.5 Look-Up Table Description

a. Radiance Calibration: Band parameters

Origin	NOAA POD and KLM Users Guide
Construction	4 x 19 per satellite, in ASCII
Usage	Define HIRS channel band central wavenumber and correction coefficients

b. Radiance Calibration: PRT Coefficients

Origin	NOAA POD and KLM Users Guide
Construction	6 x 4 per satellite (N05-N14), in ASCII 5 x 5 per satellite (N15-N17), in ASCII 7 x 5 per satellite (N15-N21), in ASCII
Usage	Define HIRS PRT count to temperature conversion coefficients

c. Radiance Calibration: Temperature prediction coefficients

Origin	Hai-Tien Lee. CISESS-MD
Construction	9 x 19 x 2, in ASCII
Usage	Define temperature prediction coefficients to estimate temperature-dependent calibration coefficients

d. HIRS/IASI/CrIS OLR Regression Coefficients

Origin	Hai-Tien Lee. CISESS-MD
Construction	HIRS: 10 x 6500 per satellite, in ASCII format IASI: OLR_COEF_TABLE 7x305x650; PRED_TABLE 3x305, in IDL Save format CrIS: OLR_COEF_TABLE 7x305x650; PRED_TABLE 3x305, in IDL Save format
Usage	Define OLR regression model

e. Inter-satellite Bias Adjustment

A controlled copy of this document is maintained in the CDR Program Library.
Approved for public release. Distribution is unlimited.

Origin	Hai-Tien Lee. CISESS-MD
Construction	22 x 1 in ASCII
Usage	Define OLR bias adjustments (Wm^{-2})

f. Coefficients for OLR Diurnal Models

Origin	Hai-Tien Lee. CISESS-MD
Construction	3 x 144 x 72 Binary
Usage	Define OLR diurnal models

g. Time markers for OLR CDR time series

Origin	Hai-Tien Lee. CISESS-MD
Construction	7 x 720 ASCII
Usage	Define time markers for the monthly mean: center, bower and upper bounds

3.4.6 Parameterization

None.

3.4.7 Algorithm Output

Name	Monthly OLR CDR
Content	Global 2.5°x2.5° gridded monthly mean OLR time series from 1979 to the presently processed month
File Format	NetCDF4
Specific Data	OLR-Monthly_v03r00_s197901_e202312_c202411151500.nc (example file name for the annual NetCDF data file that contains Daily OLR fields for the year 2023)
Physical Unit	Wm^{-2}
Size	22 MB (for 45 years of monthly mean data)

4. Test Datasets and Outputs

4.1 Test Input Datasets

The test input datasets consist of the entire HIRS level1b data available as of Sept. 1, 2017.

4.2 Test Output Analysis

4.2.1 Reproducibility

To test the reproducibility of the Rejuvenated OLR CDR package against the baseline version of the v02r07 processing system at CICS, the differences of the monthly mean values were examined. The Rejuvenated OLR CDR package is the one to be used for official production of v02r07, while evaluations/validations were conducted with the output from the baseline version. Therefore, we need to examine the reproducibility for the code packages

Figures 6 and 7 summarize the statistics of the comparison by showing the average and standard deviation of the global monthly mean OLR differences between the rejuvenated and the baseline v02r07 processing packages. Most of the differences are related to the increased number of retrievals in the rejuvenated version, which improves the ability to construct of the “super data”. (The super data is a processing unit that contains HIRS earth-view scan lines encompassed by the warm/cold calibration scans at both ends.) In the baseline version, many super data were abandoned when there are some missing scans.

The range of the average and standard deviation of the global monthly OLR differences are within expectation that we consider the reproducibility is maintained.

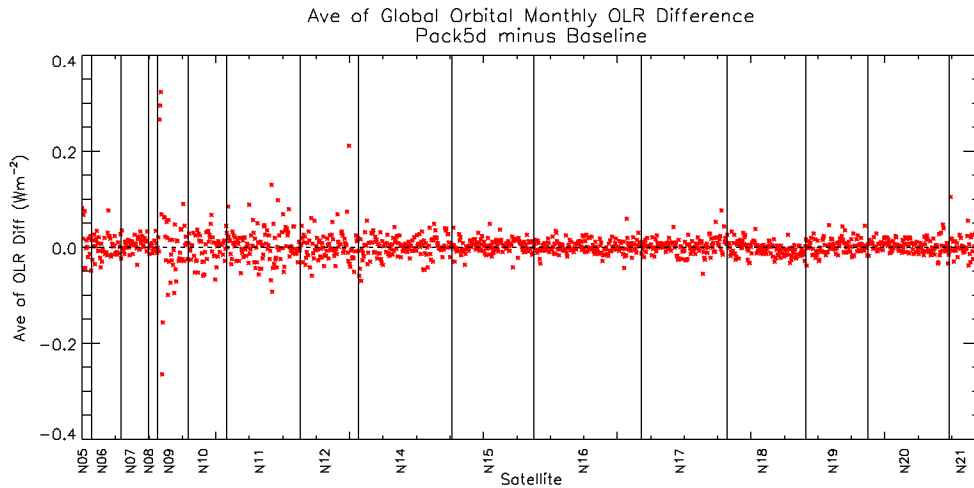


Figure 6 Differences of Global mean OLR CDR between the Rejuvenated and the baseline version of the v02r07 code packages. (Rejuvenated version is labeled as “Pack5d”)

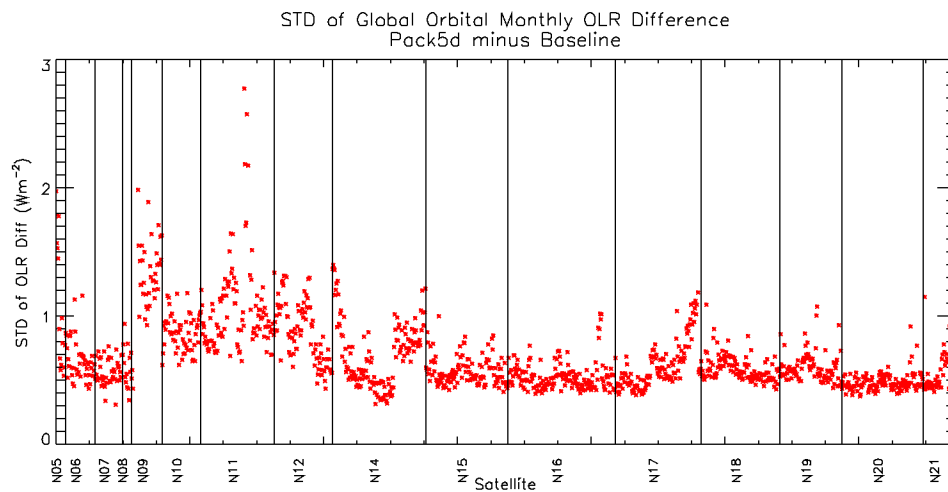


Figure 7 Similar to Figure 6 but is for the standard deviation of the global monthly mean OLR differences.

4.2.2 Precision and Accuracy

The precision and accuracy of the OLR CDR product are determined by the comparisons to the reference broadband OLR products, currently the CERES EBAF Ed4.0 OLR product.

The current assessment of the OLR CDR is to have a precision within 2 Wm^{-2} and an accuracy of about 2 Wm^{-2} , relative to the CERES EBAF Ed.4.2 OLR product

Figure 8 summarizes the OLR differences between v3.0 Monthly OLR CDR and the CERES EBAF Ed4.2 for about 24 years data record from March 2000 to Dec 2023, on the monthly basis. The mean and standard deviation of the OLR differences indicate that for

the majority of the globe, the Daily OLR CDR is within $\pm 2 \text{ Wm}^{-2}$ relative to the EBAF with standard deviations within 2 Wm^{-2} . Note that the CERES OLR product has an uncertainty of about 1.5%.

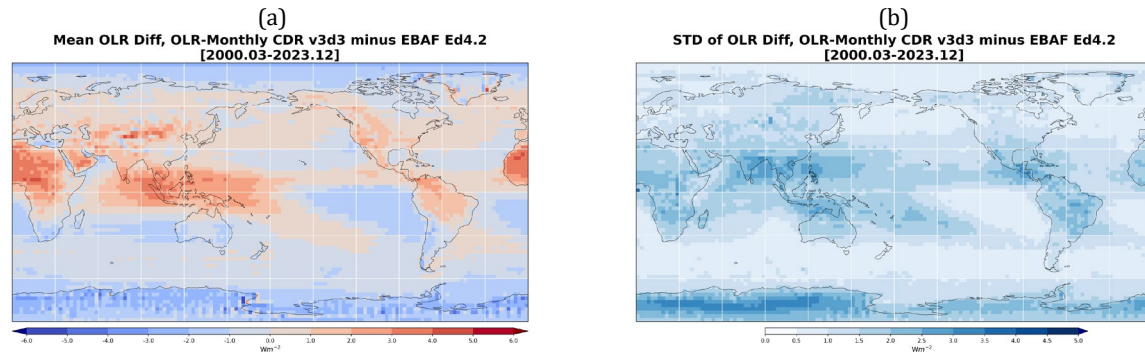


Figure 8. The OLR differences between Daily OLR CDR v02R00 and the CERES EBAF Ed4.2 on the monthly basis: (a) mean OLR differences, and (b) standard deviation of the OLR differences, over the period of March 2000 to December 2023. Most areas in (a) are shown to have relative biases to within $\pm 2 \text{ Wm}^{-2}$, with standard deviations within 2 Wm^{-2} in most areas.

The time series of the global average of OLR differences between Monthly OLR CDR v03R00 and the CERES EBAF Ed4.2 is shown in **Figure 9**. The global statistics indicate that the Daily OLR CDR has a relative bias of about 0.1 Wm^{-2} and a precision of about 1.9 Wm^{-2} relative to the CERES EBAF OLR.

The comparisons of the monthly OLR anomalies between the v3.0 Monthly OLR CDR and the CERES EBAF Ed4.2 OLR product over the global and tropical domains are shown in **Figure 10**. The OLR anomaly variability of the two products tracks each other in excellent synchronization and superb agreement in magnitude. The trends of the OLR anomalies differences for the global and the tropical domains are $0.147 \pm 0.035 \text{ Wm}^{-2}/\text{decade}$ and $0.479 \pm 0.053 \text{ Wm}^{-2}/\text{decade}$, at 2-sigma level. For the Terra-Aqua co-existent period, 2004-2023, the trend of the OLR anomalies differences for the global and the tropical domains become $0.014 \pm 0.027 \text{ Wm}^{-2}/\text{decade}$ and $0.240 \pm 0.039 \text{ Wm}^{-2}/\text{decade}$, at 2-sigma level, that satisfies the stability requirement for climate quality data: $\pm 0.3 \text{ Wm}^{-2}/\text{decade}$.

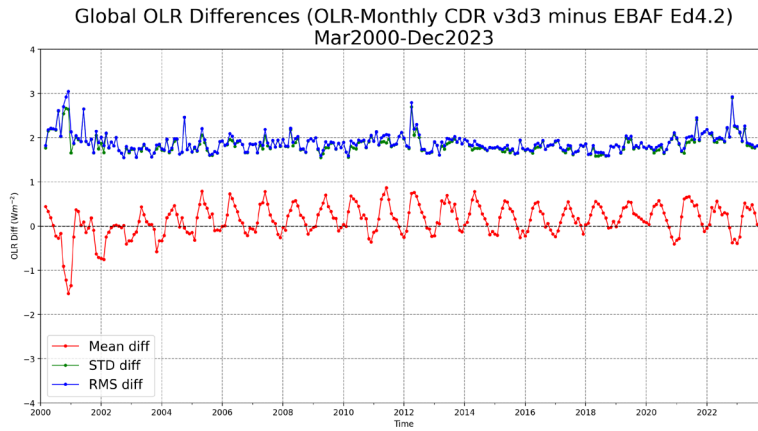


Figure 9 Mean, Std and RMS differences of the global mean OLR, Monthly OLR CDR v3.0 minus EBAF Ed4.2.

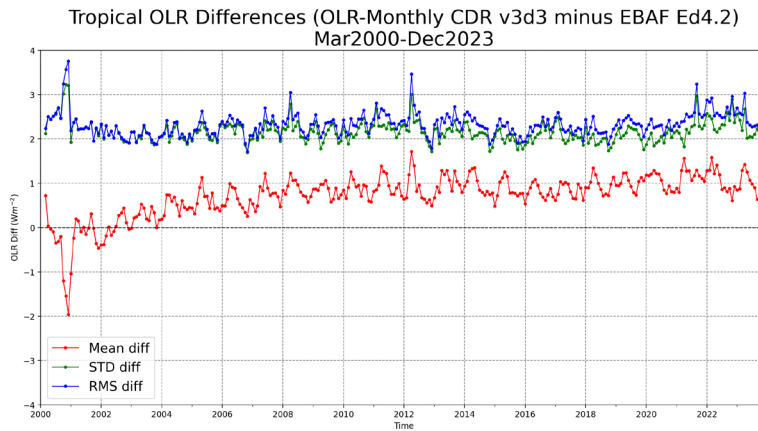


Figure 10 Mean, Std and RMS differences of the tropical mean OLR, Monthly OLR CDR v3.0 minus EBAF Ed4.2.

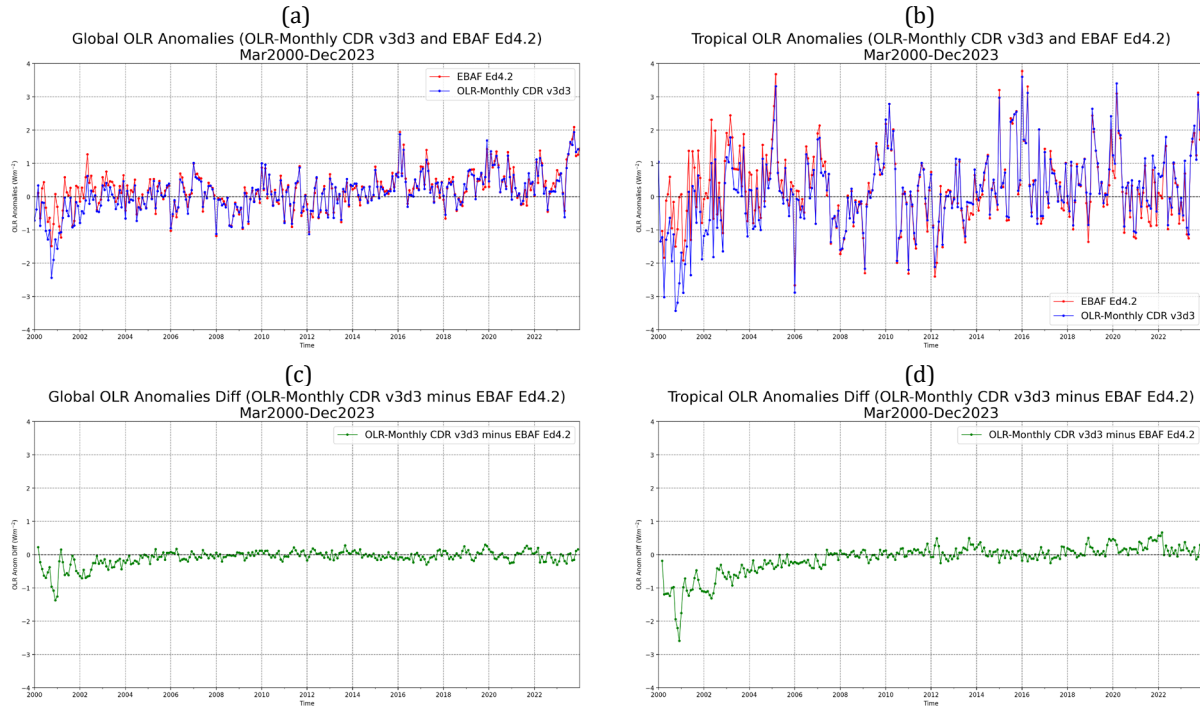


Figure 11 Comparison of OLR anomalies between the Monthly OLR CDR v3.0 (blue) and the CERES EBAF Ed4.2 (red) OLR products over the (a) global and (b) tropical 20S-20N domains. The differences of the OLR anomalies for global and tropical domains are shown in (c) and (d), respectively.

4.2.3 Error Budget

The possible sources of error for OLR CDR derivation are listed in Table 4.3. The best estimates of their magnitude of errors are given. Note that those errors cannot be aggregated in a simple form.

Table 9 Error sources and best estimated magnitude for OLR CDR production.

Error Sources	Magnitude of Errors	Prospective Improvements
Radiance Calibration	bias at $\sim 0.5^\circ\text{K}$	<ul style="list-style-type: none"> ○ non-linear calibration method; ○ estimate of post-launch spectral response function;
OLR retrieval	RMS errors ~ 2 to 3 Wm^{-2}	<ul style="list-style-type: none"> ○ More accurate OLR estimation model, e.g., band-by-band
Intersatellite calibration	biases at ~ 1 to 2 Wm^{-2}	<ul style="list-style-type: none"> ○ Scene dependent bias adjustments; ○ More consistent OLR models across HIRS instrument versions;
Navigation (Local Zenith Angle error in N14)	$\sim 30^\circ$	<ul style="list-style-type: none"> ○ Redo HIRS1b navigation ○ Assume constant satellite view angles ○ construct empirical estimation of LZA
Temporal integral	?	<ul style="list-style-type: none"> ○ Use of geostationary observations to better describe the OLR diurnal variation

5. Practical Considerations

5.1 Numerical Computation Considerations

- Endian

The OLR CDR Production Package assumes IEEE big-endian environment.

- Precision

The codes can be run under either 32-bit or 64-bit mode.

- Parallelization

This production package is considered not computationally intensive that explicit parallelization is not performed.

5.2 Programming and Procedural Considerations

None.

5.3 Quality Assessment and Diagnostics

Quality flags and automatic diagnostics will be implemented.

5.4 Exception Handling

Gridder.f90

The equator crossing time cannot be determined when there are insufficient numbers of near equator observations in a given orbit file. The ECT will be considered missing and is assigned to -1 when that is the case returning to calling routine. The monthly mean ECT determination (in grid_OLR.f90) will skip those missing ECT during averaging.

OLR_monthly_integral.sh

In initial design that this script will exit when the number of OLR FOV retrieval output files for a given satellite is less than 15. Currently this threshold is defined at 0, effectively removing this criteria. Be cautious when HIRS-1b data is only partially available in a given month.

OLR_monthly_integral.f90

This program will stop when the read statement for reading the coefficients of the OLR diurnal models encounters error. Currently there is no error handling of such incident. The monthly mean OLR ASCII output file will not be generated when this happens. (And the netCDF packaging will not generate any result either.). Human interruption is required in this case to resolve the directory/file location error.

OLR_CDR_nc4_batch.f90

The packing of NetCDF parameters is subject to error check, by subroutine `check_err`. The program will exit if any errors were detected. This will cause failure in the generation of NetCDF product file. This condition will be written to the process log and human interruption will be required.

5.5 Algorithm Validation

- Summary

The production and validation of the OLR CDR Ver.02 Rev.00 (time series 1979-2003) is described in Lee et al. (2007). This validation has shown that the OLR CDR time series has stability comparable to that of the Earth Radiation Budget Satellite (ERBS) non-scanner OLR measurements, at about 0.3 Wm^{-2} per decade. Globally, HIRS OLR agrees with CERES with an accuracy to within 2 Wm^{-2} and a precision of about 4 Wm^{-2} .

The assessments for the revised OLR CDR v02r07 against the updated CERES OLR EBAF Ed4.0 product show significant improvements over those previously established. The over accuracy is now assessed to be at about 2.5 Wm^{-2} . The most important improvement is in the removal of the spurious trend present in the v02r02 product.

For the new v03r00 Monthly OLR CDR, validations have been carried out against the broadband OLR products references with the results shown in Section 4.2.2. The validation assessments show that the Monthly OLR CDR time series has a stability satisfying the climate quality data requirement, at about 0.3 Wm^{-2} per decade for 2004-2023 period. Globally, Monthly OLR CDR agrees with CERES EBAF OLR product within 2 Wm^{-2} with a precision of about 2 Wm^{-2} . This is well within the CERES OLR uncertainty, of about 1.5%.

- Validation Strategy

The HIRS/IASI/CrIS OLR retrieval and the monthly OLR CDR product can be evaluated with the radiative flux measurements from broadband instruments, including the ERBS non-scanner, ERBE scanners, and CERES scanners.

For the instantaneous retrieval accuracy assessment, HIRS, IASI and CrIS OLR retrieval at HIRS FOV is compared against the CERES Level-2 single scanner footprint (SSF) product, where the broadband radiance measurement is converted to the total flux at FOV level.

The inter-comparison of the OLR CDR product with other OLR products and model simulations is a continuing effort. Multiple sets of inter-comparisons enable us to identify problems in the data sets that are otherwise difficult to affirm. These exercises can raise the confidence level of the validation assessments.

5.6 Processing Environment and Resources

Processing System Configuration

- CPU: MacPro 3.3 GHz 12-Core Intel Xeon, 160 GB 2933 MHz DDR4 memory
- Operating System: Mac OS X 14.7 (Sonoma)
- Programming Language: Fortran 95, IDL 8.9.0, Python 3.11
- Compilers: gfortran 14.2.0
- External Libraries: NetCDF 4.9.2.1
- Working space (for 1979-2024 input and output): about 16 TB.

6. Assumptions and Limitations

- Radiative Transfer Model Simulations

The OLR regression models were constructed with a set of radiative transfer model simulations. As being statistical models, they are assumed to be representative for global application in all sky conditions. Scene-dependent errors might be traceable to this assumption and modeling improvements would be necessary to eliminate such errors.

- Intersatellite Calibration

The inter-satellite bias adjustments are determined with the collocated observations during the overlapping period for two satellites. Since the majority of collocations occur in the polar regions that the derived biases may not be representative for other climate zones. The revised OLR regression models v3.0 have significantly improved the consistency between OLR retrieved from different versions of HIRS instruments and reduced local zenith angle and latitude dependencies that have been identified in previous models. Nevertheless, the possibility of scene-dependent inter-satellite biases still exists that becomes a possible source of errors for stability and trend.

- OLR Diurnal Model

The accuracy of monthly mean temporal integration is limited by the temporal sampling rate and integration method employed. The current OLR CDR production uses climatological OLR diurnal models to estimate monthly mean. It assumes, on the monthly mean basis, that the magnitude of inter-annual/decadal variation in OLR diurnal cycle is much smaller than that of the OLR diurnal cycle itself. This is quite valid over land but may not always hold true over the ocean, e.g., the large change in cloudiness in equatorial Pacific during El Niño years.

The use of OLR diurnal models indeed helps to reduce artifacts caused by the orbital drift and changes of observation time, but more accurate temporal integration could be attained with OLR observed/estimated from geostationary satellites.

- Navigation

The OLR CDR production uses HIRS level-1b data as the primary input. It assumes that the navigation parameters, including the coordinates and viewing geometry for the earth FOV locations, are correct. There are known errors: incorrect local zenith angle data in NOAA14 post March 1999 would degrade the OLR retrieval quality. Such errors need to be dealt with offline.

6.1 Algorithm Performance

The OLR retrieval will be performed when the radiances from the required HIRS channels are available, otherwise, the OLR retrieval will not be performed. There are possible degradation paths for the OLR retrievals using different sets of prediction

channels. However, these degradation paths are yet to be explored and currently undefined.

6.2 Sensor Performance

- Radiometric Calibration

The OLR CDR production performs radiance calibration following McMillin method. A set of coefficients is used in predicting calibration coefficients. This is to introduce instrument temperature dependence for the interpolation of the calibration coefficients between two calibration cycles. These coefficients may require updates when the instrument temperatures have shifted significantly from the existing samples.

- Radiometric Noise

The OLR CDR production package examines the quality flags of the HIRS level-1b data to determine if OLR retrieval can be performed. The OLR retrieval will still be performed when the sensor radiometric noise is higher than the instrument specification, but the quality flag is not turned on. There are several problems in the recent HIRS instruments since NOAA-15 that requires ad hoc examination to determine better quality control for OLR retrieval purpose.

- Spectral Response Function

The spectral response function has a role in the radiance calibration and in the radiance simulation. The accuracy of OLR estimation depends on the radiative transfer model simulations of the OLR flux and the HIRS radiances. Errors will be introduced if the pre-launch response function characterization is incorrect, or the response functions have changed post-launch.

- Instrument Scanning Alignment

There are known errors in the HIRS scanning operation on NOAA15 and 16. It is currently believed that the scanning is off by one scanning step position, in both satellites. Correction in the navigation parameters has already been applied in the level-1b data. Users should be aware of this error and use these data more cautiously.

7. Future Enhancements

7.1 Enhancement 1 – Reprocessing of IASI and CrIS OLR

Currently the input for IASI and CrIS OLR retrievals are the operational products: IASI L1C and CrIS SDR. The reprocessing of IASI and CrIS radiance products are an ongoing and active research area that reprocessed data sets are being released through various agencies. It is potentially that the accuracy and continuity of IASI and CrIS OLR retrievals would be improved when derived with the reprocessed observational data.

7.2 Enhancement 2 – Metop-SG IASI-NG

The Next-Generation of IASI to be flown on Second-generation of Metop satellites series will soon be available. The IASI-NG improved both the sampling frequency and spectral resolution of the IASI hyperspectral radiance spectrum data. The adaptation of IASI OLR algorithm for the IASI-NG instrument will be performed. The processing system shall be ready to take in the IASI-NG Level1C data when it becomes operationally available.

7.3 Enhancement 3 – CrIS OLR Retrieval

The magnitude of the intersatellite calibration adjustments for CrIS OLR are unexpectedly large, at about 1.4 Wm^{-2} . The cause of the relatively large bias in CrIS OLR is currently unclear, but possibly a programming bug. Investigation in the CrIS OLR algorithm implementation is necessary.

7.4 Enhancement 4 – OLR Diurnal Model

The empirical OLR diurnal model currently in use was derived with monthly composite of 1979-2009 data, with OLR regression model v2.2. Re-deriving and update the diurnal models with the OLR regression model v3c6 with 1979-present data will improve the consistency for the monthly temporally integral procedure and potentially improve the accuracy the Monthly OLR CDR product.

8. References

- Ba, M., R. G. Ellingson and A. Gruber, 2003: Validation of a technique for estimating OLR with the GOES sounder. *J. Atmos. Ocean. Tech.*, **20**, 79-89.
- Cressman, G. P., 1959: An operational objective analysis system. *Mon. Wea. Rev.*, **87**, 367-374. Ellingson, R. G. and M. Ba, 2003: A study of diurnal variation of OLR from the GOES Sounder. *J. Atmos. Ocean. Tech.*, **20**, 90-98.
- Ellingson, R. G. and J. C. Gille, 1978: An infrared radiative transfer model. Part 1: Model description and comparison of observations with calculations. *J. Atmos. Sci.*, **35**, 523-545.
- Ellingson, R. G., H.-T. Lee, D. Yanuk and A. Gruber, 1994: Validation of a technique for estimating outgoing longwave radiation from HIRS radiance observations, *J. Atmos. Ocean. Tech.*, **11**, 357-365.
- Ellingson, R. G., D. J. Yanuk, H.-T. Lee and A. Gruber, 1989: A technique for estimating outgoing longwave radiation from HIRS radiance observations. *J. Atmos. Ocean. Tech.*, **6**, 706-711.
- Harries, J.E., J.E. Russell, J.A. Hanafin, et al., 2005: The geostationary Earth Radiation Budget Project. *Bull. Amer. Meteor. Soc.*, **86**, 945-960.
- Gruber, A., R. G. Ellingson, P. Ardanuy, M. Weiss, S.-K. Yang and S. N. Oh, 1994: A comparison of ERBE and AVHRR longwave flux estimates. *Bull. Amer. Meteor. Soc.*, **75**, 2115-2130.
- Gruber, A., and T. S. Chen, 1988: Diurnal variation of outgoing longwave radiation. *J. Climatol.*, **8**, 1-16.
- Gruber, A., H.-T. Lee and R. G. Ellingson, 2004: Climate monitoring with HIRS outgoing longwave radiation data. The 13th Conference on Satellite Meteorology and Oceanography. September 20-23, 2004, Norfolk, VA.
- Jackson, D. L., J. J. Bates and D. P. Wylie, 2003: The HIRS Pathfinder radiance data set (1979-2001). Proceedings of 12th Conference on Satellite Meteorology and Oceanography, Long Beach, California, February 10-13, 2003.
- Jacobowitz, H., L. L. Stowe, G. Ohring, A. Heidinger, K. Knapp, and N. R. Nalli, 2003: The Advanced Very High-Resolution Radiometer Pathfinder Atmosphere (PATMOS) climate dataset: a resource for climate research. *Bull. of Amer. Meteo. Soc.*, **84**, 785-793.

- Knapp, K. R., S. Ansari, C. L. Bain , M. A. Bourassa , M. J. Dickinson , C. Funk , C. N. Helms , C. C. Hennon, C. Holmes , G. J. Huffman , J. P. Kossin, H.-T. Lee , A. Loew , G. Magnusdottir, 2011: Globally gridded satellite (GridSat) observations for climate studies. *Bulletin of American Meteorology Society.*, 893-907. (doi: 10.1175/2011BAMS3039.1)
- Lee, H.-T., 2023: CDRP-RPT-1442 Rev 0 OLR - Daily Technical Note (01B-21) (DSR-1840). NCEI Climate Data Record Program
- Lee, H.-T., 2023: CDRP-RPT-1443 Rev 0 OLR - Monthly Technical Note (01B-06) (DSR-1841). NCEI Climate Data Record Program
- Lee, H.-T., A. Gruber, and J. Lee, 2010b: Operational Generation of the HIRS Outgoing Longwave Radiation Climate Data Record. Scientific Data Stewardship Annual Meeting. Sept 14-15, 2010. NCDC, Asheville, NC
- Lee, H.-T., A. Heidinger, A. Gruber, and R. G. Ellingson, 2004a: The HIRS Outgoing Longwave Radiation product from hybrid polar and geosynchronous satellite observations. *Advances in Space Research*, **33**, 1120-1124.
- Lee, H.-T., I. Laszlo, and A. Gruber, 2010a: ABI Earth Radiation Budget - Outgoing Longwave Radiation. NOAA NESDIS Center for Satellite Applications and Research (STAR) Algorithm Theoretical Basis Document (ATBD)
- Lee, H.-T., 2011: Sustainability of HIRS OLR Climate Data Record from Research to Operation. First Conference on Transition of Research to Operations: Successes, Plans and Challenges. 91st AMS Annual Meeting, Seattle, WA, January 23-27, 2011.
- Lee, H.-T., R. G. Ellingson, and A. Gruber, 2010: Development of IASI outgoing longwave radiation algorithm. *Proceedings of the 2nd IASI International Conference*, Annecy, France, January 25-29, 2010.
- Lee, H.-T. and R. G. Ellingson, 2013: HIRS OLR Climate Data Record - Production and Validation Updates. *Proceedings of the 2012 International Radiation Symposium (IRS'2012)*. AIP Conf. Proc., 1531, 420 (2013); doi: 10.1063/1.4804796
- Lee, H.-T., and R. G. Ellingson, 2013: Improvement of HIRS OLR CDR inter-satellite calibration using IASI observations. 2013 joint EUMETSAT/AMS Meteorological Satellite Conference, 16-20 September 2013, Vienna, Austria (Poster)
- Lee, H.-T., 2014: Daily OLR Climate Data Record – A challenge to homogenize operational satellite observations for climate applications. EGU General Assembly 2014.
- Lee, H.-T., 2014b: Daily OLR Climate Data Record – A challenge to homogenize operational satellite observations for climate applications. EGU General Assembly 2014, 27 April – 2 May 2014, Vienna, Austria

Lee, H.-T., C. J. Schreck, K. R. Knapp, 2014c: Generation of the Daily OLR Climate Data Record. 2014 EUMETSAT Meteorological Satellite Conference, 22-26 September 2014, Geneva, Switzerland

GCOS: <http://www.wmo.int/pages/prog/gcos/index.php?name=EssentialClimateVariables> (as of July 19, 2011)

NOAA Polar Orbiter Data (POD) User's Guide: 1998 version available online at <http://www.ncdc.noaa.gov/oa/pod-guide/ncdc/docs/intro.htm> as of July 18, 2011.

NOAA KLM User's Guide: Feb. 2009 version available online at <http://www.ncdc.noaa.gov/oa/pod-guide/ncdc/docs/intro.htm> as of July 18, 2011.

Ohring, G., A. Gruber and R. G. Ellingson, 1984: Satellite determinations of the relationship between total longwave radiation flux and infrared window radiance. *J. climate & Appl. Meteor.*, **23**, 416-425.

Schreck, C. J., H.-T. Lee and K. Knapp, 2018: HIRS Outgoing Longwave Radiation—Daily Climate Data Record: Application toward Identifying Tropical Subseasonal Variability. *Remote Sens.* 2018, 10, 1325; <https://doi.org/10.3390/rs10091325>

Turner, E. C., H.-T. Lee and S. F. B. Tett, 2015: Using IASI to simulate the total spectrum of outgoing long-wave radiances, *Atmos. Chem. Phys.*, 15, 6561-6575, doi:10.5194/acp-15-6561-2015.

Warner, J. X. and R. G. Ellingson, 2000: A new narrowband radiation model for water vapor absorption. *J. Atmos. Sci.*, **57**, 1481-1496.

Wielicki, B. A., B. R. Barkstrom, E. F. Harrison, R. B. Lee, G. L. Smith, and J. E. Cooper, 1996: Clouds and the Earth's Radiant Energy System (CERES): An Earth Observing System Experiment. *Bull. Amer. Meteor. Soc.*, **77**, 853-868.

Wong, T., B. A. Wielicki, R. B. Lee, III, G. L. Smith, K. A. Bush, and J. K. Willis, 2006: Re-examination of the Observed Decadal Variability of Earth Radiation Budget using Altitude-corrected ERBE/ERBS Nonscanner WFOV data. *J. Climate*.

Young, D. F., P. Minnis, D. R. Doelling, G. G. Gibson and T. Wong, 1998: Temporal Interpolation Methods for the Clouds and the Earth's Radiant Energy System (CERES) Experiment. *J. Appl. Meteorology*, **37**, 572-590.

Appendix A. Acronyms and Abbreviations

Acronym or Abbreviation	Definition
ABI	Advanced Baseline Imager
AVHRR	Advanced Very High Resolution Radiometer
CATBD	Climate Algorithm Theoretical Basis Document
CDR	Climate Data Record
CERES	The Cloud and the Earth's Radiant Energy System
CrIS	Cross-track Infrared Sounder
ECT	Equator Crossing Time
EOS	Earth Observing System
ERBE	Earth Radiation Budget Experiment
ERBS	Earth Radiation Budget Satellite
EUMETSAT	European Organization for the Exploitation of Meteorological Satellites
FOV	Field of View
GCOS	Global Climate Observing System
GEO	Geosynchronous orbit
GERB	Geostationary Earth Radiation Budget Experiment
GOES	Geostationary Operational Environment Satellite
GSIP	GOES Surface and Insolation Product
IASI	Infrared Atmospheric Sounding Interferometer
HIRS	High-resolution Infrared Radiation Sounder
LUT	Lookup Table
LZA	Local Zenith Angle
Metop	Meteorological Operational Polar Satellite
NASA	National Aeronautics and Space Administration
NESDIS	National Environmental Satellite, Data, and Information Service
NCEI	National Centers for Environmental Information
NOAA	National Oceanic and Atmospheres Administration
POES	Polar-orbiting Operational Environmental Satellite
RTM	Radiative Transfer Model
SDR	Scientific Data Record
STD	Standard Deviation
TIROS	Television Infrared Observation Satellite
TOA	Top of Atmosphere
TOVS	TIROS Operational Vertical Sounder
WMO	World Meteorological Organization

Appendix B. IASI and CrIS OLR Retrieval Algorithms

The hyperspectral OLR estimation principle and IASI and CrIS OLR retrieval algorithms are explained here.

The total outgoing longwave radiative flux density, OLR, is the integral of the spectral fluxes over the thermal radiation spectrum,

$$\text{OLR} = \int F_\nu d\nu \quad (\text{B.1})$$

The spectral flux F_ν at frequency ν is the integral of the normal specific radiances at the top of the atmosphere, z_t , over the hemispheric dome related to the local zenith angle θ and azimuthal angle ϕ ,

$$F_\nu = \int_0^{2\pi} \int_0^{\pi/2} I_\nu(z_t; \theta, \phi) \cos\theta \sin\theta d\theta d\phi \quad (\text{B.2})$$

Frequency-dependent Spectral Angular Models (SAM), can be constructed to approximate the spectral flux integral, for a radiance observation at local zenith angle θ , such that,

$$F_\nu \cong \text{SAM}_\nu(I_\nu(z_t; \theta)) \quad (\text{B.3})$$

There are two principles that make the spectral flux estimation possible with the spectral angular models:

1. **Inter-Frequency Correlations** - Radiances at one frequency are strongly correlate with radiances at another with similar absorption features.
2. **Intra-Frequency/Angle Correlations** - Using “absorption strength” as surrogate to “optical path length”, spectral flux integration can be estimated with radiances at selected angles (as in Gaussian quadrature)

Previous works can be found in Lee, Ellingson & Gruber (2010); Turner, Lee & Tett (2015).

The IASI OLR algorithm is a 3-predictor multiple linear regression model in quadratic forms, whereas the predictors are natural log of IASI radiances aggregated to 10 cm^{-1} intervals in 650-2500 cm^{-1} range. Note that the IASI radiance observations over 2500-2760 cm^{-1} are not used due to possible solar contamination.

$$\begin{aligned} \log(F_\nu) = & a_0(\nu, \theta) + a_1(\nu, \theta) x_1(\nu, \theta) + a_2(\nu, \theta) x_2(\nu, \theta) + \\ & a_3(\nu, \theta) x_3(\nu, \theta) + a_4(\nu, \theta) x_1^2(\nu, \theta) + \\ & a_5(\nu, \theta) x_2^2(\nu, \theta) + a_6(\nu, \theta) x_3^2(\nu, \theta) \end{aligned} \quad (\text{B.4})$$

where

$$x_\nu = \log(I_\nu(\theta)) \quad (\text{B.5})$$

with the frequency and zenith angle-dependent regression coefficients a 's.

Figure B1 shows the correlations between the spectral flux and radiance at different zenith angles. The strongest correlations can be seen near 53° and this is related to the diffusivity approximation. The spectral locations with strong absorption features tend to produce weaker correlations for zenith angles outside vicinity of 53° , and this is where the Intra-frequency/angle correlations become useful for the spectral flux estimation.

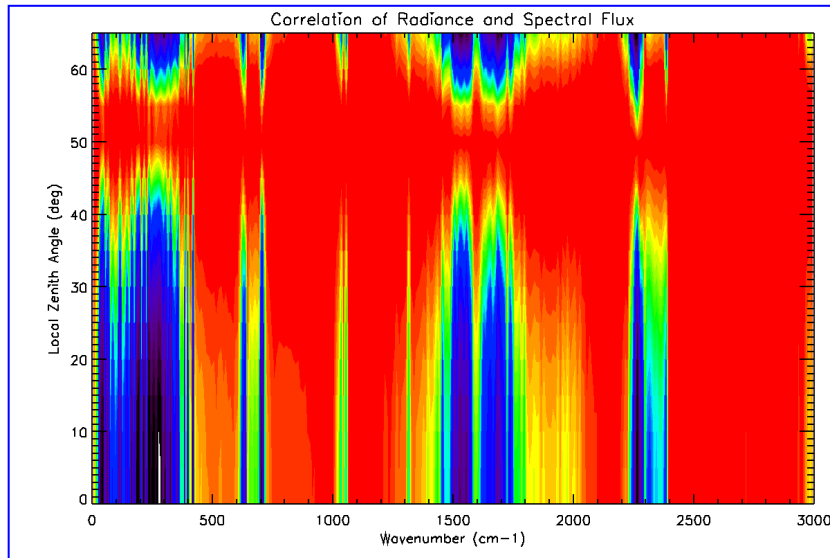


Figure B1 Correlation between spectral fluxes and radiances at different local zenith angles.

Figure B2 shows the selection of the predicting radiances for the estimation of spectral fluxes at each 10 cm^{-1} wavenumber band. The estimate of the IASI OLR estimation errors is shown in **Figure B3**, where the rms total estimation errors range from $0.13 - 0.47 \text{ Wm}^{-2}$. The far infrared (FIR) spectral domain, $0-650 \text{ cm}^{-1}$ contributed most of the errors, due that the FIR spectrum is not directly observed and the spectral fluxes are not well correlated to radiance observations at most of the angles.

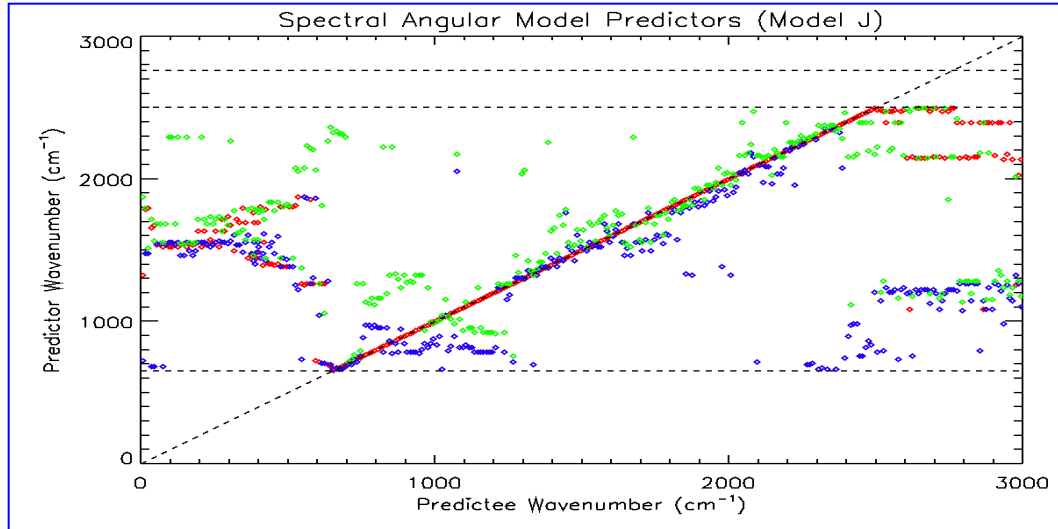


Figure B2 Selections of predicting radiances (y-axis) for the estimation of spectral fluxes (x-axis) at each 10 cm-1 wavenumber band, with IASI radiances observations in 650-2500 cm-1 range. There are three selected predicting radiances wavenumbers at each spectral band, represented by colors red, blue and green.

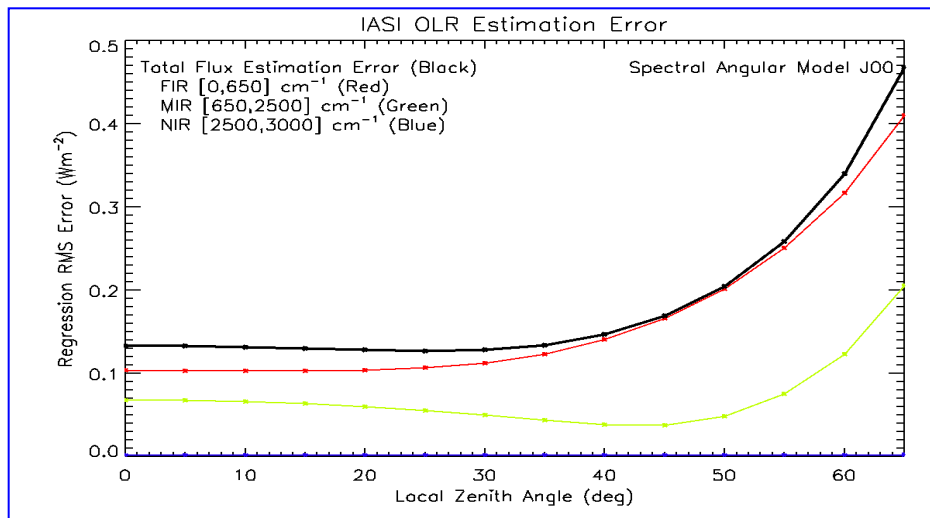


Figure B3 RMS regression errors for the total OLR estimation, as a function of the observing local zenith angle, range from 0.13 - 0.47 Wm-2, and are dominated by flux estimation errors from the “FIR” spectral domain.

Note that the CrIS OLR algorithm shares the similar estimation principle and model design, except some part of the mid thermal spectrum not directly observed by CrIS would be estimated from the observed CrIS radiances with similar principle.

Appendix C. HIRS OLR Regression Model (v3.0) for Daily OLR v2.0 and Monthly OLR v3.0 CDR

Up to Daily OLR CDR v1.2 and Monthly OLR CDR v2.7, the HIRS OLR were estimated by the HIRS OLR regression models whose regression coefficients were determined from a set of 3200 atmospheric profiles based on Phillip Soundings.

For the Daily OLR CDR v2.0 and Monthly OLR CDR v3.0 upgrades, the HIRS OLR model form has changed to include two additional predicting channels (**Eq. C.2**) and the regression coefficients were instead determined with a set of HIRS radiances simulated by IASI hyperspectral observations with the corresponding IASI estimated OLR fluxes. The main objective of this approach is to improve OLR retrieval consistency between the narrow-band the hyperspectral instruments.

Previous v2.7 HIRS OLR Regression Model form:

$$OLR = a_0 + a_1N_3 + a_2N_7 + a_3N_8 + a_4N_{11} + a_5N_8^2 + a_6N_{11}^{0.5} + a_7N_{12}^{0.5} \quad (C.1)$$

The new v3.0 HIRS OLR Regression Model form (for Daily v2.0 and Monthly v3.0):

$$OLR = a_0 + a_1N_3 + a_2N_7^{0.1} + a_3N_8 + a_4N_8^{0.5} + a_5N_{11} + a_6N_{11}^{0.5} + a_7N_{12}^{0.5} + a_8N_9 + a_9N_5 \quad (C.2)$$

The simulation data set comprises the IASI-simulated HIRS radiances and IASI-estimated OLR, for all 16 HIRS instruments onboard TIROS-N to Metop-B/01, derived from two-day worth of IASI hyperspectral radiance observations in Jan 1st and July 1st, 2010. The RMS regression errors is reduced to 0.86 Wm⁻² (compared to 1.67 Wm⁻² when using the previous regression model) for the M02 HIRS instrument. (see **Fig. C1**)

Fig. C2 show the regression residual distribution pattern, as a function of the estimated OLR. The uniformity, flatness of the residual distribution is desired. It can be clearly seen that the HIRS OLR retrieval random errors are dependent on the fluxes (scene dependent), while the errors in the new model have achieved the desired uniformity.

The examination of OLR retrieval errors as a function of latitude are shown in **Fig. C3**. The distribution of regression residuals from the new model is shown to be uniform over latitudes. This is supported by the evaluation with the collocated CERES Terra SSF Ed.4A OLR data. Compared to the latitudinal dependency of the “HIRS minus CERES” differences in the old model, the new model has clearly improved the latitudinal agreements with respect to CERES product.

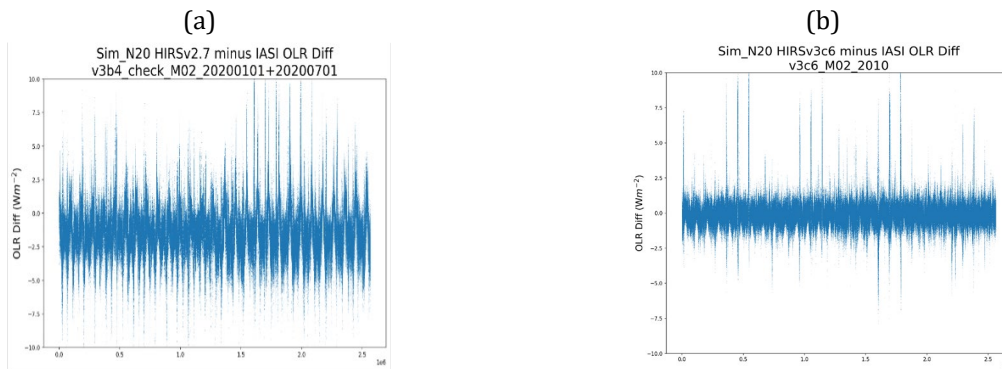


Figure C1 RMS regression residual errors of the total OLR estimation for the (a) v2.7 and (b) v3.0 models. The drastic reduction in residual errors indicate the improved consistency between HIRS OLR and IASI OLR retrievals.

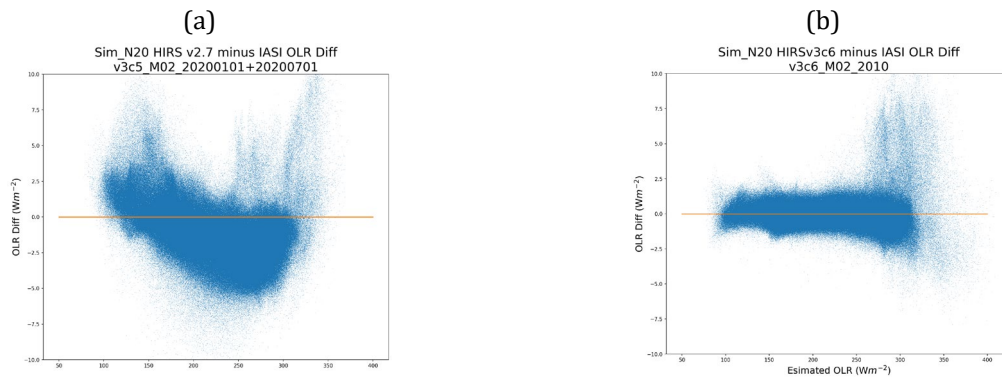


Figure C2 Regression residuals of the (a) v2.7 and (b) v3.0 models, as a function of estimated OLR (as in typical regression residual plot). The significantly better residual distribution pattern from the new model is evidence of the OLR retrieval consistency that can be achieved between HIRS and IASI.

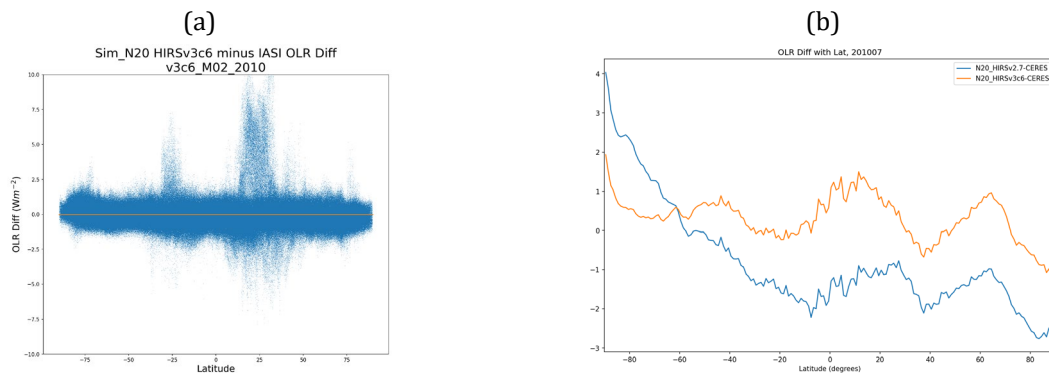


Figure C3 (a) Regression residuals of the new models as a function of latitude, (b) validation of HIRS OLR retrieval against CERES Terra SSF Ed.4A data in July 2010. The latitudinal dependence in HIRS OLR minus CERES SSF differences from new v3.0 model (orange) can be seen to be much improved over the previous v2.7 model (blue curve) are shown in panel (b).

Validation of IASI and HIRS OLR retrievals

The new v3.0 HIRS OLR model adopts M02 IASI derived OLR as radiometric reference. It is necessary to show the accuracy of the IASI OLR retrievals and to assess the performance of the HIRS OLR retrievals from the new regression model.

Figs C4/C5 show the OLR retrieval comparisons at the field of view level, by collocating IASI and HIRS (v3.0) with CERES Terra SSF data respectively, over Jan and Jul 2015. Similar validations were performed with CERES Aqua SSF product and other permutations.

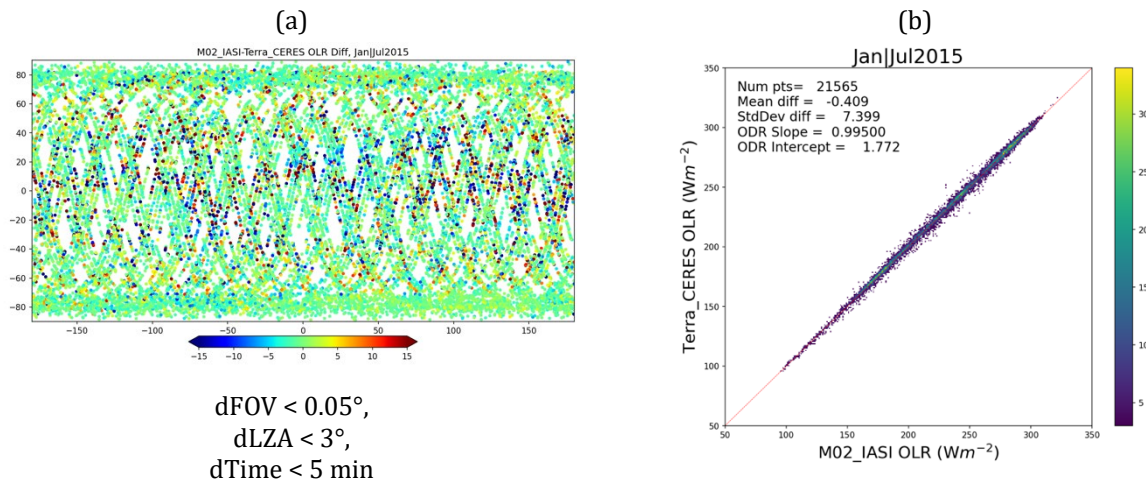


Figure C4 (a) IASI and CERES OLR differences at collocation with the given constraints for Jan + July 2015 observations (b) validation of M02 IASI OLR retrieval against CERES Terra SSF Ed.4A data in Jan + July 2015.

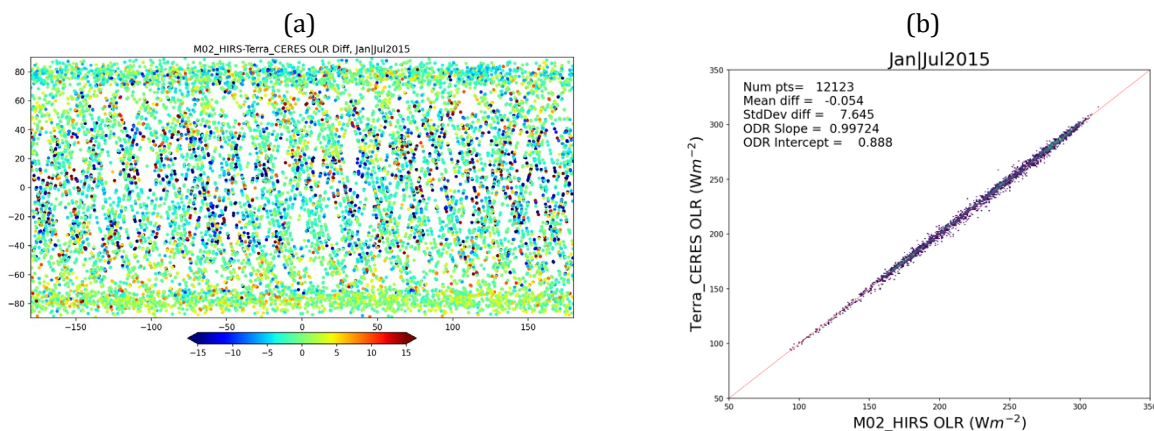


Figure C5 (a) M02 HIRS v3.0 OLR and CERES OLR differences at collocation with the given constraints for Jan + July 2015 observations (b) validation of M02 HIRS v3.0 OLR retrieval against CERES Terra SSF Ed.4A data in Jan + July 2015.

The statistics OLR retrieval validation comparisons are summarized in **Table C1**. The biases of HIRS v3.0 and IASI OLR retrievals relative to CERES are within the uncertainty of the CERES instantaneous OLR product, at about 1.5%. The standard deviation of the OLR differences those compared against to CERES Aqua SSF are 4.5 to 5 Wm^{-2} , which are comparable to that between CERES Terra and Aqua themselves. For pairs that have collocations extended into lower latitudes, e.g., M02 and Terra, the larger Std Diff are related to the larger OLR at lower latitudes and higher variability associated with clouds.

These validation results provide strong confidence that adapting M02 IASI OLR as the absolute radiometric references level serves well for the new OLR CDR construction purposes. And the new HIRS OLR v3.0 retrievals, with their regression models derived directly referencing to M02 IASI OLR, are maintained at the same radiometric level. This paves a solid ground for time series stability.

Table C1 OLR retrieval validations for permutations between HIRS, IASI and CERES instruments for Jan+Jul 2015.

	Mean Diff	Std Diff	N	Std Err	ODR Slope
M02_IASI - Terra_SSF	-0.41	7.40	21565	0.050	0.9950
M02_IASI -Aqua_SSF	-0.33	4.59	14734	0.038	0.9942
M02_HIRS - Terra_SSF	-0.05	7.64	12123	0.058	0.9972
M02_HIRS - Aqua_SSF	0.07	4.77	8382	0.052	0.9953
Terra_SSF - Aqua_SSF	0.14	4.60	88912	0.015	0.9946
M01_IASI - M02_IASI	-0.14	13.48	48651	0.061	0.9992

Appendix D. Inter-satellite Calibration For HIRS, IASI and CrIS OLR Retrievals

The inter-satellite calibration is determined from collocated OLR retrievals at instantaneous, field of view (FOV) level. OLR retrievals from all pairs of satellites/instruments were collocated for their entire overlapping period except those excluded by QC, with the following criteria:

- within 0.05° between center of FOVs
- within 3 minutes between observing times (except a few pairs that the limit is extended to 60 minutes such that collocation becomes possible)
- within 3° between observing local zenith angles
- Limit to observations with Local zenith angles within 45°

Several experiments were carried out with different approaches of inter-satellite calibration methods and/or different propagation paths and they lead to very similar results. The one codenamed “v3d6” is adopted for the new CDR production.

Prior to this Daily v2.0 and Monthly v3.0 upgrade, the NOAA-9 HIRS OLR retrieval is adopted as the absolute radiometric references, due to the previous works that have tied the NOAA-9 HIRS OLR to the ERBE broadband OLR product well. For this upgrade, the Metop-A (M02) IASI OLR retrieval will be serving as the absolute radiometric reference, for its higher accuracy in OLR retrieval and well-maintained on-orbit calibration. OLR retrieval validation (see Appendix E, Fig. E4) provided clear evidence that justifies this decision.

The v3d6 inter-satellite calibration adjustments are shown in **Fig. D1**. The differences in HIRS spectral response functions between the pre-launch measurement versus those in-orbit are the main sources for the relative biases. The relative biases between IASI and CrIS OLR retrievals are unusually large but cannot yet be explained.

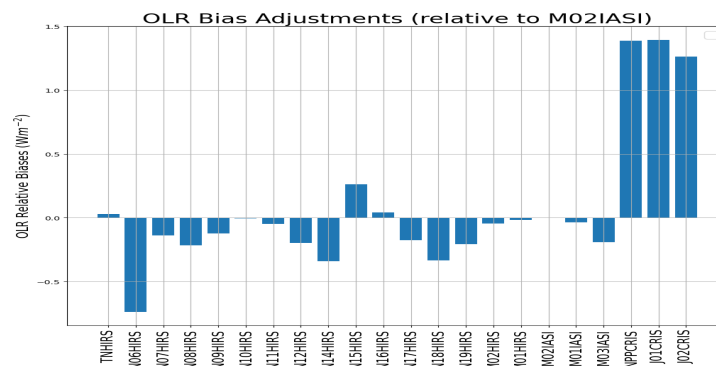


Fig. D1 Inter-satellite calibration adjustments to be deducted from the OLR retrievals of the given satellite-instrument.